Modelling of Mouse Spermatogonial Stem Cell Niche for Designing 3D scaffolds for in vitro Spermatogenesis

Inigo J

Department of Biotechnology and Medical Engineering

National Institute of Technology Rourkela

Department of Biotechnology and Medical Engineering

National Institute of Technology Rourkela

Prof. Mukesh Kumar Gupta
Associate Professor

May 30, 2016

Supervisor's Certificate

This is to certify that the work presented in the dissertation entitled *Modelling of Mouse Spermatogonial Stem Cell Niche for Designing 3D scaffolds for in vitro Spermatogenesis* submitted by *Inigo J*, Roll Number 214BM2025 is a record of original research carried out by him under my supervision and guidance in partial fulfillment of the requirements of the degree of *Master of Technology* in *Biotechnology*. Neither this dissertation nor any part of it has been submitted earlier for any degree or diploma to any institute or university in India or abroad.

Prof. Mukesh Kumar Gupta
Supervisor

Declaration of Originality

I, *Inigo J,* Roll Number *214BM2025* hereby declare that this dissertation entitled *Modelling of Mouse Spermatogonial Stem Cell Niche for Designing 3D scaffolds for in vitro Spermatogenesis* presents my original work carried out as a *Post Graduate* of NIT Rourkela and, to the best of my knowledge, contains no material previously published or written by another person, nor any material presented by me for the award of any degree or diploma of NIT Rourkela or any other institution. Any contribution made to this research by others, with whom I have worked at NIT Rourkela or elsewhere, is explicitly acknowledged in the dissertation. Works of other authors cited in this dissertation have been duly acknowledged under the sections "Reference". I have also submitted my original research records to the scrutiny committee for evaluation of my dissertation.

I am fully aware that in case of any non-compliance detected in future, the Senate of NIT Rourkela may withdraw the degree awarded to me on the basis of the present dissertation.

May 30, 2016

NIT Rourkela

Inigo J

Acknowledgement

I would like to express my deep gratitude to my Project Supervisor and Guide, **Dr. Mukesh Kumar Gupta**, Professor and Head, Department of Biotechnology and Medical Engineering, NIT Rourkela for providing me the opportunity to work under his guidance and supporting me at all the stages of this work. I am highly obliged to him for providing me with all necessary academic and administrative facilities during the project work.

It would not have been possible for me to understand and exploit the modelling environment without the insights of **Dr. B. P. Nayak** and **Dr. P. Balasubramaniam**. Im highly grateful to them.

I thank **Dr. Indranil Bannerjee** and **Dr. SS Ray** for their constructive criticisms during viva voce sessions that helped me identify and solve most of my technical mistakes.

I am grateful to **Er. Senthil Kumar, Er. Praveen Kumar, Er. Krishna Kumar Ramajayam** and **Dr. Rakesh Bhaskar** for their incessant support, inspiration and constructive criticism throughout my research.

I extend my regards to all my lab-mates **Er. Gopalakrishnan, Er. Sovan Das, Er. Bijayalaxmi Sahoo** and **Er. Tanushree Patra** for helping me avail the facilities of a rich and fruitful environment in a peaceful way.

I am thankful to my senior, **Er. Gokulnathan Kasinathan** for his advice and support during my odd times.

Above all, I would like to thank my parents for their unlimited support and love towards strengthening my carrier.

30 May, 2016

Rourkela

Inigo J

Roll No: 214BM2025

Abstract

The homeostasis of male genitalia in mammals is maintained by a group of stem cells called spermatogonial stem cells (SSCs) which replenishes worn out cells in the testicular tissue. In mouse, these cells are housed by specialised tubular structures called seminiferous tubules. The SSC niche is found dispersed on the basal lamina, which is a two dimensional extracellular matrix along the circumference of seminiferous tubules. The Myoid, Sertoli and Leydig cells support SSCs while self-renewal and differentiation. The self-renewal and migration of SSCs takes place along the lateral direction and differentiation occurs medially towards the lumen of seminiferous tubules. The differentiation and self-renewal occurs in a cycle with each cycle possessing 12 stages of seminiferous epithelium. The self-renewal and commitment for differentiation of stem cells occurs from stages X – VIII of seminiferous epithelium. A Matlab^{TM} program was developed to simulate the behavior of SSCs in their niche within the seminiferous tubules with logical rules. The migration, self-renewal and differentiation of SSCs was modelled according to the logical parameters provided by researches over the past century. The behavior of SSCs in their niche was assumed to be dependent on cell density in that niche area. The SSCs responded to the density stress imposed on them by their neighbouring cells which forced them migrate into a space with lower stress. Similarly, division and differentiation was also controlled by density stress through various thresholds. The model outcome was validated with literature. The model predicted that there was 12 A_{single} cells, 15 A_{paired} cells and 19 $A_{aligned}$ cells per 1000 Sertoli cells in the niche of mouse. With these metrics in concern, a biopolymer scaffold was prepared by using alginate to mimic the testicular tissue. Polymerisation was performed by the process of ionotropic gelation with $CaCl_2$ as the crosslinker. Channels of diameter from 100 µm to 250 µmm were obtained in the anisotropic gel. The tubular nature of the scaffold mimicked seminiferous tubules in dimension. Physiochemical characterization like SEM, FTIR, Mechanical analysis of the scaffold was done on the scaffold.

Keywords: ***SSC simulation; Mathematical Modelling; Calcium alginate gels; Ionotropic gelation; Scaffold***

Contents

List of Figures

List of Tables

CHAPTER 1

INTRODUCTION

All mammalian tissues are believed to contain stem cells which replenishes the worn out cells and thus, maintain the homeostatic balance. All the mature / terminally differentiated cells of the body that organise themselves and carry out various functions of the body arise from a group of undifferentiated and immature cells termed stem cells. These stem cells have various characteristic properties like self-renewal, mitosis and long term conservation of naïve genome without epigenetic changes (Yamanaka et. al., 2013). Self-renewal is the division of one stem cell into two daughter cells that resemble the parent in all the way, thereby, producing two more stem cells. This is helpful in maintaining a constant stem cell number in a particular environment of the stem cell called niche. Potency is the property of the stem cell to differentiate into various types of cells that mature terminally and help in carrying out various functions of the body.

The sperm cells are terminally differentiated cells that transfer genetic material to the egg during fertilisation. These cells arise from a colony of stem cells called spermatogonial stem cells (SSCs). SSCs in turn arise from primordial germ cells (PGCs) during perinatal testes development. PGC specification occurs in extra-embryonic ectoderm These PGCs proliferate and colonise the genital ridges (De Rooij et. al., 1998). In the male genital ridges, they are supported by Sertoli cells which are somatic cells. PGCs and Sertoli cells together form solid strands of cells called the seminiferous cord. Later, during development, these cords develop lumen to form seminiferous tubules. Spermatogonial stem cells are present in testes inside the seminiferous tubule (De Rooij et. al., 1997).

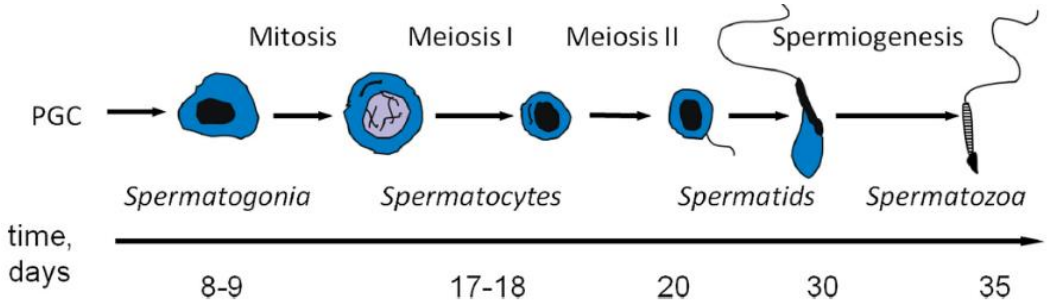

Figure 1: Time course of spermatogenesis (Khill et. al.,2004)

1.1. THE SEMINIFEROUS TUBULE

Seminiferous tubules consist of germ cells and somatic cells. The extracellular matrix of seminiferous tubule is called the basal lamina. The Myoid cells wrap the basal lamina. Leydig cells are present in the interstitial space between the tubules. Sertoli cells form tight junctions within the tubules. These tight junctions separate the tubule into two compartments. One is the basal compartment which is limited by the basal lamina, the other is the adluminal compartment that extends till the lumen of the seminiferous tubule. The basal compartment acts as a boundary between Spermatogonia and other differentiating cells. All spermatogonia (A_s, A_{pr}, A_{al}) occupy the basal compartment. They are localised along the circumference of the tubule on the basal lamina and are in contact with the Sertoli cells. Nagano et. al.,1999 demonstrated that the preferential localisation of transplanted SSCs on the basal membrane is close to blood vessels at the surface. Upon differentiation, the cells leave the basal compartment and move to the adluminal compartment when they are at preleptotene cell stage. Mammalian SSCs have a characteristic motility along the two dimensional axis of the basal lamina, unlike those of lower organisms such as drosophila where they are non-motile (Yoshida et al., 2007) and were dispersed throughout the length of the tubule. The stem cells are motile along the XY Direction and differentiation takes place along the Z direction.

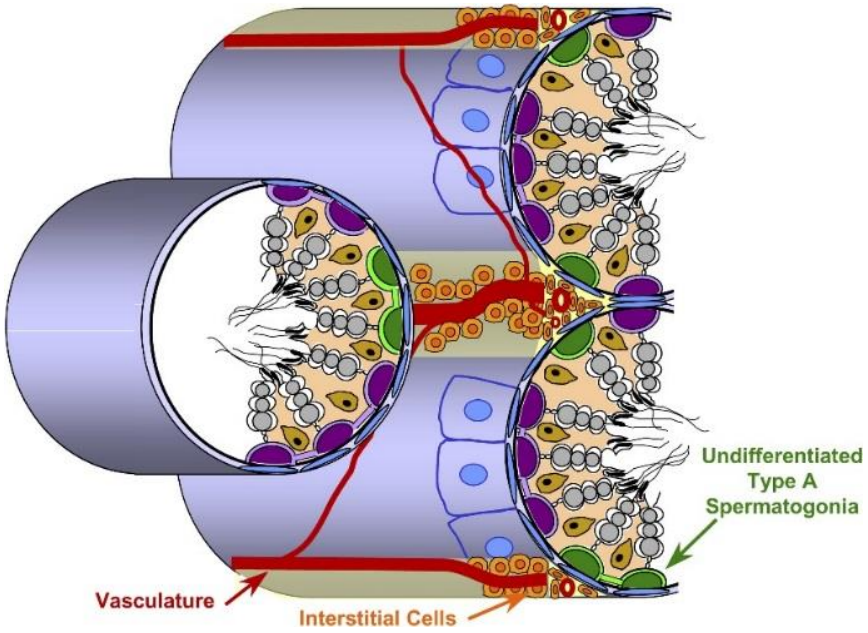

Figure 2: 3 Dimensional Reconstruction of SSC Niche imaging (Shetty et. al, 2007).

1.1.1. THE CYCLE OF MOUSE SEMINIFEROUS EPITHELIUM

Spermatogenesis takes place in the basal lamina of the seminiferous tubule, supported by leydig, sertoli and myoid cells. The most accepted model of spermatogenesis involves the Asingle (A_s), Apaired (A_{pr}) and Aaligned (A_{al}) cells that has stemness and either differentiate into primary and secondary spermatocytes or self-renew in order to repopulate the niche. The process of spermatogenesis is a cyclic process with one cycle having many stages. In each stage of the cycle, a particular batch of cells will synchronously divide and differentiate. Mouse spermatogenesis contains 12 such stages.

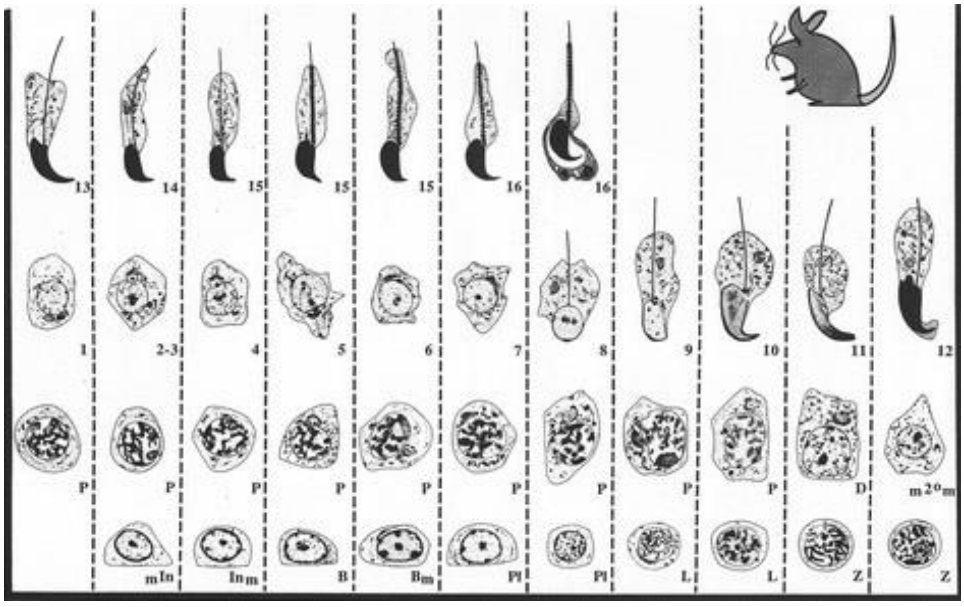

Figure 3: Stages of the cycle of mouse seminiferous epithelium (Boer et.al.,2015)**.**

According to Oakberg et.al., (1956) there are 12 stages in a single wave of mouse seminiferous epithelium. During each stage, unique population of germ cells and spermatocytes occupy the length of the tubule. Type A spermatogonia which constitute the germline stem cells are present in all the stages of the cycle. Intermediate spermatogonia are found in stages II, III and IV. Type B spermatogonia are not found in any stage other than IV, V and VI. When a single cycle of spermatogonial proliferation and differentiation completes, new spermatocytes appear at stages VI and VII. They form a layer below the older spermatocytes closer to the basement membrane. Thus, through the rest of the cycle, there are two layers of cells found in the seminiferous tubule. The newly formed cells are closer to the basement membrane. The first layer of spermatocytes is found at the end of stage VII and at the beginning of stage VIII. It enters leptotene at stage VIII. These leptotene cells are found at

stages VIII, IX and partially in X. At the end of stage X, Zygotene begins. The pairing will be complete when stage XII starts. Pachytene begins at stage XII and the spermatocytes remain in pachytene still Stage X of the next cycle. At stage XII, diplotene appears and diakinesis occurs at stage XII. The secondary spermatocytes immediately divide into spermatids at stage XII. Thus, spermiogenesis involves more than one spermatogonial cycle. There are 16 steps of spermatid development. The first 8 steps overlap with the steps 13 to 16. Thus, in the tubule stage I, the second layer of spermatid is in its 13^{th} step of development. At the same time, the older spermatids are differentiated into mature spermatozoa. The spermatids in their 14^{th} step of maturation are found in stage II and III of the tubule. Tubules at stage IV, V and VI are occupied by maturing spermatozoa at their 15^{th} step of development. Stages VII and VIII of epithelial tubule are occupied by spermatozoa at their 16^{th} step of development. At stage VIII, mature sperm is released into the lumen of the seminiferous tubule.

1.2. MODELLING OF BIOLOGICAL PROCESSES

Modelling and simulation of various biological systems is a challenging field of research. Drastic development of computational processing capacity and availability of huge readable data on biological systems have enabled the modelling and approximate to accurate prediction of biological systems with complex computational algorithms (Sujansky et.al.,2001). To understand the complex biological systems like organelles, cells, tissues and even the whole organism, only refining the molecules out of the cell and performing tests on them would not suffice. It also involves a deep understanding of how these molecules interact within themselves and within their surroundings. Modelling of biological components and their processes allows researchers to investigate how these components are regulated and also provides information about the interactions of these components within themselves. Since the data on biological processes are very huge After the development of high speed computational resources and availability of huge databases, process modelling based on these data is feasible (Aittokallio et.al.,2006).

1.2.1. BIOLOGICAL COMPLEXITIES

In order to model a biological process, one has to understand various complexities of that particular system. The parameters and functions must be provided in such a manner that they satisfy these complexities and don't compromise the way the biological systems actually function (Hinegardner et.al., 1983). The key complexity of a biological system is 'Chance' (Pavé et.al, 2007). Right from the broad picture of phenotypes to the narrowed areas of molecular interactions that lead to that particular phenotype, there can be chance events that happen, so that no two components in a biological system are fully identical. Even daughter cells that arise from the same parent are not identical in terms of molecular composition and functions. They might be similar, but, not identical. It is due to stochastic noises in the biological processes that affect each and every outcome of the process thereby introducing at least meagre changes in the system that might not be perceivable.

The second complexity arrives from the fact that knowing the information about a single structural component alone would not necessarily give us complete information about the functional counterpart. For example, a single gene can give rise to many functional proteins depending on how it is spliced. So, knowing the genetic code alone without any information about the splicing will not be enough to predict the phenotype of that gene. Thus, it is to be noted that a biological function is the outcome of interaction of many biological components (Morange et.al.,2001).

The third complexity is that information about the dynamic molecular interactions governing the complex behaviour of organisms is scarce (Van Regenmortel et.al.,2004). Since the complexities cannot be controlled in most of the cases, one of the most promising approaches to solve these complexities is through analysing the process data and do an approximate prediction about the outcomes of the process. This can then be extended to formulating a hypothesis and then either proving it or disproving it with the help of mathematical and statistical approaches.

1.2.2. NATURE OF BIOLOGICAL DATA

Heterogeneity:

Biological data is heterogeneous (John C. Wooley et.al., 2005). It might be a sequence information on genomic and protein data. It can be a graph or a chart representing the signal pathways. It can also be geometric information about the structure of a molecule that relates it to its function. It can also be a spatial information on structure of a molecule or also patterns on the molecule that provides it with its function.

Accuracy:

Acquisition of biological data is not always accurate because of background effects and noises (Sloutsky et. al.,2013). Background effects are not caused by the organism in consideration, but, is caused by the contemporary environmental factors. Many factors like sample preparation type, chemical usage, etc. can give rise to modifications in the data acquired. Instrumentation and experimental errors can also give rise to variations in data accuracy (John C. Wooley et.al.,2005).

Organisation:

The data will be useless if it is inaccessible to others because of their heterogeneity and size. Hence, in order to increase the accessibility of the data, it is better to extract the information from the data and organise them according to their utility. The data obtained must allow itself to be organised and arranged as in a database so that future reference to the required information is possible. Thus, the data obtained must be curated and should be integrable (Birkland et.al.,2006). After preprocessing the data, it should ready for use in developing a model (Moussouni et.al.,2013). A model is a close representation of a working system. When it comes to modelling mathematical data, it is classified into: i) Deterministic models, where the input and output variables are fixed; ii) Stochastic models, where the variables are probabilistic; iii) Dynamic models, where the variables possess time varying interactions and iv) Static models, where, the variables are considered independent of time (Imboden et.al.,2012).

1.2.3. BUILDING MODELS FOR BIOLOGICAL PROCESSES

Biological process modelling can be either quantitative or logical or both. Quantitative models involve obtaining crude data from the processes and pre-processing them to make the data readable. Then, a hypothesis is formulated and it is tested through various statistical methods. Logical models define mathematical relationships in the form of logical rules on the obtained parameters thereby modelling the system's behavior (Wynn et.al.,2012). The process of building a model involves multiple iterations which involves a definite number of variables. The mathematical relationships between them and the parameter values are selected and simulations are performed to either reproduce observations or to forms predictions. According to the behaviour and complexity of the system during various iterations, novel variables can be introduced into the model. Thus, the complexity of the model could be made comparable to the complexity of the system by increasing the number of iterations and thereby increasing the number of significant variables (Le Novère et. al.,2015).

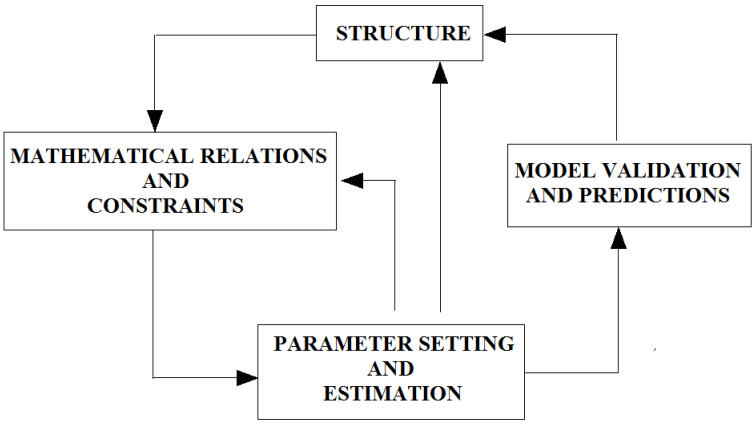

Figure 4: Building mathematical model of biological processes (Le Novère et. al.,2015)

The first layer of a model is to determine the biological entities that are to be represented in the model. The number of entities to include depends on the problem statement and the available data to declare the parameters. Approximation is always preferred over accuracy to solve complex models. Approximation reduces the complexities in a data and helps in saving computational resources. A biological effect may be caused by many components. But, it is a general approximation that 80% effects are caused by 20% components (Jankowski et.al.,2013). Hence, certain constraints are ignored in the model according to the problem statement. The next layer involves finding the interactions between the selected entities. The final layer involves characterising and quantifying the relationships.

CHAPTER 2

REVIEW OF LITERATURE

In mammals especially mouse and ram, the spermatogonial stem cells were named as A-single (A_s) SSCs (Oakberk,1971, De Rooij et.al.,1998). These A_s cells either undergo cytokinesis to form two new cells or may result in incomplete cytokinesis so that there is an intercellular cytoplasmic bridge with which the two daughter cells are connected so as to form A-paired spermatogonial cells (A_{pr} cells). The Apr cells then divide into chains of A-aligned spermatogonia (A_{al} cells). A_{al} cells can be of 4, 8 or 16 cells that are connected by intercellular cytoplasmic bridges. The Apr and A_{al} cells are considered to be committed for differentiation and are the amplifying portion of Spermatogenesis. A_{al} cells then differentiate into A1 spermatogonia at stage VII/VIII of seminiferous epithelium in mouse, the first generation of differentiating spermatogonia. A_1 spermatogonia undergo a series of six or more differentiations into A_2, A_3, A_4, intermediate and B spermatogonia. B spermatogonia give rise to primary spermatocytes (De Rooij, et.al.,1983).

In mammals, the SSCs are located in the basal lamina and are sequestered by the Sertoli cell barrier so that they do not move closer to the tubule lumen. This makes the SSC niche (Chiarini-Gracia et.al.,2003) a two dimensional, one cell thick layer within the tubular area (Russel et.al.,1990, De Rooij et.al.,2013). Studies were carried out by Brinster et. al.,1994 where a method of transplanting mouse SSCs from a fertile testis to an infertile testis was discussed and the infertile testis was found to take part in spermatogenesis following SSC transplantation (SSCT). Nagano et. al.,1999 conducted experiments by wherein all SSCs in a mouse testis were depleted by γ-radiation and then populating it with fresh SSCs. It was found that, after 4 hours, some of the newly seeded SSCs were bound to the sertoli cells and only a very few were floating in the lumen of the seminiferous tubules. By 1 month after transplantation, SSCs were found both adhered to the sertoli cells and also found to form a two dimensional patch on the basement membrane. Only the cells with cytoplasmic bridges were found to migrate towards the lumen.

The A_s, A_{pr} and A_{al} spermatogonia are most frequently localized in areas of the tubule basal membrane bordering on patches of interstitial tissue (Chiarini-Gracia et.al., 2003). This was confirmed later by fluorescent tagging studies on spermatogonia that showed that these

A_s, A_{pr} and A_{al} cells are localized near venules and arterioles in the interstitial area. These cells were most probably found in areas where the blood vessels branch (Yoshida et.al.,2007). Morphologically, these cells cannot be distinguished from each other. As cells can be distinguished from A_{pr} and other cells with intercellular bridges since A_s cells will be at a distance of at least 25µm from each other (Lok et.al.,1983). So, cells in pairs that have a distance of less than 25 µm may be labeled as Apr cells.

In order to model the simulation of the behavior of A_s, A_{pr} and A_{al} cells, several parameters have to be identified and incorporated into an appropriate kinetics so that the ideality of the process is achieved. The most important and the most common parameters include the niche dimension, probability of self-renewal, cell size, cell density and migration distance. The niche dimension, as inferred from the data compiled by De Rooij et.al.,2012 was set to 800 µm x 1700 µm. This was because, the circumference of the seminiferous tubule was generally found to be around 1700 µm and hence a cut along the length on the seminiferous tubule will result in a rectangle of the given dimension. An area of this sort would contain 4000 Sertoli cells. Each stem cell (A_s) is supported by 100 sertoli cells (Lok et.al.,1983, Russel et.al., 1987) and hence, this niche area should contain atleast 40 As cells. The probability of self-renewal depends on the location of the stem cells. Their preferential location near the vasculature suggests that the probability of self-renewal at these sites will be higher than other sites that don't have a vasculature branching nearby (Ellis et.al.,2011). Hence, an imaginary vasculature was drawn and along the vasculature, the probability of self-renewal was set to 90%. The probability decreased with increasing distance from the vasculature. The probability ranged from 90% to 10% within the niche depending on the distance from the vasculature. The cell sizes used were pretty straight forward: As=1, Apr=2, Aal=4, 8 and 16 depending on the length of the chain. Since, in Chinese hamsters, the Aal32 cells were nowhere to be found, A_{al16} cells will not divide further into Aal32 (Lok et.al.,1982). The cell density is one of the most important parameter since it influences the division of As spermatogonia. Cell density was never found to affect in any case the ratio of A_s, A_{pr} and A_{al} (De Rooij et.al.,1987). After division, the daughter cells were found to migrate to a location of lower cellular density. If such a low density site is not found and the density around the cell destined for mitosis is higher than a particular threshold, the cell won't divide. Cell density also influences cell migration in a similar way. Cells will try to combat contact inhibition by

migrating to the lowest density site in the niche but at the same time, they tend to remain at a distance possibly nearest to the vasculature so that they remain a stem cell. If the cells migrate away from the niche, they differentiate. The minimum distance between cells for contact inhibition was found to be 30 µm. It differs between species, but, the range happens to be between 30 and 40 µm (Jing et.al.,2009). It was also shown that the division of a stem cell is affected if there is another cell in its proximity. The threshold for a cell to affect another cell through contact inhibition was 50 µm and the division is totally inhibited if the cells are as close as 30 µm.

The kinetics of cell division has to be found so that the niche is ideally in a steady state for a number of divisions throughout the lifecycle of the organism. The first and foremost assumption and rather a possibility is that stem cell niche maintains the division to differentiation ratios of the stem cells at '1' so that the number of self-renewing stem cells is always maintained constant (De Rooij et.al.,2001). More self-renewal than differentiation would lead to increase in the number of stem cells and may gradually lead to tumor formation. Similarly, more differentiation than self-renewal would lead to the depletion of stem cells which is a very rare happening if the organism has to survive. The niche must be balanced with constant a proliferation and differentiation profile. The ratio of differentiation to division would change if there is damage to the niche that leads to the loss of stem cells. In this case, probability would incline towards the division of stem cells so that the niche is replenished. Similarly, the proliferation of stem cells increases and continues to a longer extent (beyond stage II of epithelial cycle) when the number of A_1 spermatogonia reduces by 50% (Rooij et.al.,1985). When there is a decrease in the number of stem cells, there is another possibility that the weak intercellular bridges of A_{pr} and A_{al} cells break yielding A_s cells that may either self-renew or differentiate directly in A_1 spermatogonia. These Apr cells are called potential stem cells that replenish the niche only in case of damage to the niche (Nakagawa et.al.,2010). The A_s cells formed by this mechanism are hypothesized to have a shorter life cycle and differentiate quicker than the normal A_s cells formed by self-renewal. The shorter life cycle stem cells help in maintaining the stem cell number in the niche (Nakagawa et.al.,2010). The division of A_s cells is not synchronous as shown by the Huckins- Oakberg theory (Huckins et.al.,1971, Oakberg et.al.,1971), but their differentiation is synchronous. Clements model of spermatogenesis shows that there is a reserved pool of stem cells termed

A_0 spermatogonia that remains quiescent and are rarely seen to differentiate (Clermont et.al.,1975). Also when the stem cell is being depleted, the pattern of stem cell division changes such that more number of A_s cells are produced. This is depicted in Figure 5.

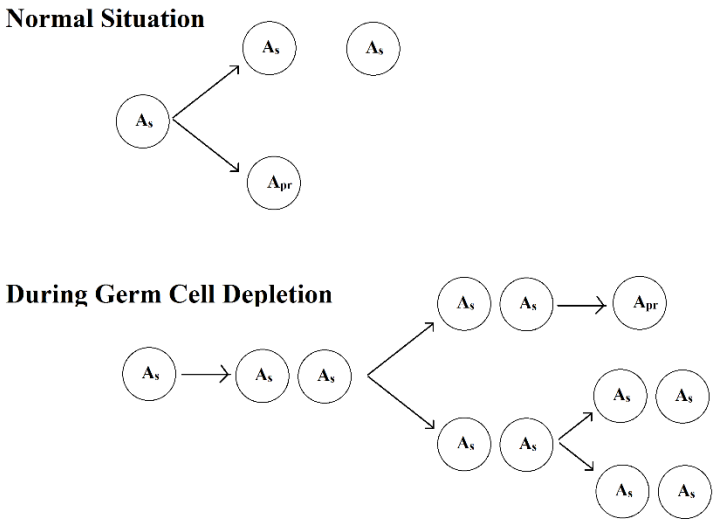

Figure 5: Condition for self-renewal. (De Rooij et.al.,2000).

Oakberg et.al.,1956 tracked the events of SSC division and differentiation and was able to determine the duration of each stage of the cycle of seminiferous epithelium in mouse. It took 8.6 days for the completion of one cycle in mouse. The duration of each stage of the epithelial cycle is given in Table 1.

Table 1: Duration of each stage of the cycle of mouse seminiferous epithelium (Oakberg et.al, 1956).

Stage	Duration (hours)
I	22.2
II	18.1
III	8.7
IV	18.6
V	11.3
VI	18.1
VII	20.6
VIII	20.8
IX	15.2
X	11.3
XI	21.4
XII	20.8

Sertoli cells and Leydig cells influence the stimulation, maintenance and progression of spermatogenesis in the form of physical support, junctional complexes or barriers and biochemical stimulation in the form of growth factors or nutrients. Sertoli cells control the progression of spermatogonia to spermatozoa with direct contact or controlling the environment mileu within the seminiferous tubule (Russell et.al.,1980). Leydig cells secrete testosterone that steers the differentiation of spermatozoa into spermatocytes by influencing the anterior pituitary of hypothalamus (McLachlan et.al.,1996). The seminiferous tubule serves as the niche where the influence of Sertoli cells and Leydig cells steer the process of spermatogenesis. Seminiferous tubules are thoroughly isolated from the various chemical cues inside the testis by an established blood-testis barrier (Hess et.al.,2008).

Damage to seminiferous tubule, hormonal imbalance, genetic mutations and dysfunction of spermatogonial cells and other cells could lead to infertility disorders. Because of the above malfunctions, the germ cells find it difficult to progress into differentiation. In vitro spermatogenesis could be an appropriate solution for this problem (Lee et.al.,2006). But, fully efficient systems for successful spermatogenesis in vitro are still not accomplished (Reuter et.al.,2012).

Tissue engineering has provided us with great possibilities of mimicking in vivo environments in vitro. Three Dimensional (3D) scaffolds have been promising in forming efficient mimics by simulating nearly accurate in vivo environments. Stem cells were cultured invitro and then were implanted into seminiferous tubules that provide the niche to develop spermatids from the SSCs (Sato et.al.,2012). Hence, 3D culture systems that mimic seminiferous tubules could possibly be the solution for efficient and complete spermatogenesis to happen invitro. The diameter of seminiferous tubule ranges from 80 µm to 300 µm in mammals (Mehraein et.al.,2011, Morales et.al.,2004, Whillis et.al.,1954). SSCs have been reported to self-renew in scaffolds that are not tubular provided the proper factors and nutrients are given (Eslahi et.al.,2013). But, did not differentiate beyond elongated spermatid stage to form the sperm in vitro. The possible cause for it might be the factors and hormones provided in the 3D scaffold. But, it could also be the 3D environment provided to the stem cells in vitro. No study has been made to culture the SSCs in 3D biopolymer scaffolds that mimic the seminiferous tubule in its structure, though such scaffolds were

produced for differentiating vascular cells. Hence, it is postulated that in vitro spermatogenesis can be made possible with a 3D environment that mimics the seminiferous tubule.

Creating a 3D environment that mimics the seminiferous tubule is a challenging task. Seminiferous tubules have a diameter of about 80 - 300 µm. Hence, the scaffold to be created should be having tubules with similar diameter. Yamamoto et. al.,2009 created honeycomb shaped 3D scaffolds for growing vascular cells. He used alginate as the biopolymer and Calcium chloride as the cosslinker for the gelation process. The gelation took place in an ordered manner because of ionotropic gelation. Calcium chloride made channels in the sodium alginate during gelation whose diameter can be adjusted by optimising the concentration of sodium alginate solution and the concentration of calcium chloride. Channels of diameter ranging from 60 µm to 400 µm can be made through this process.

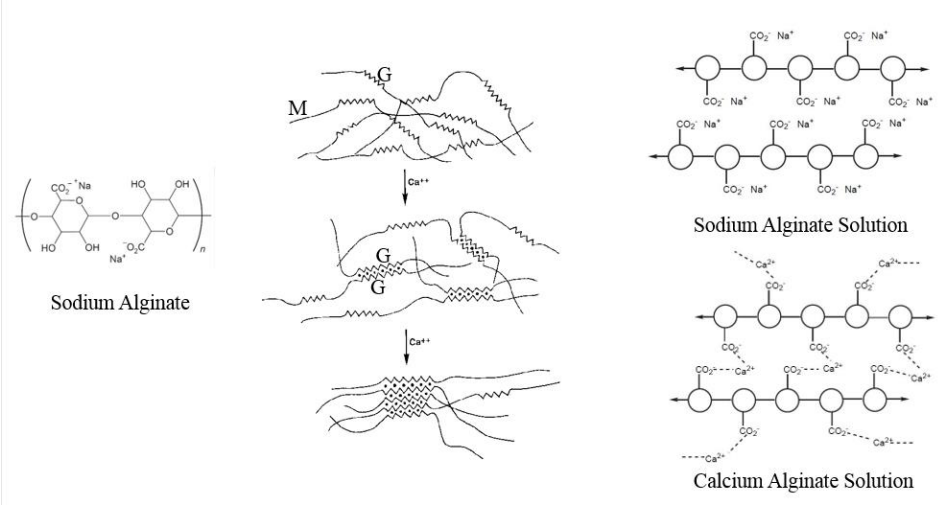

Figure 6: Structure of Sodium Alginate and Calcium Alginate (McHugh et.al.,1987)

Alginate is an anionic heteropolysaccharide made of (1-4)-linked b-D-mannuronic acid (M units) and a-L-guluronic acid (G units). They are normally available as powdered form linked with monovalent sodium ions. When two GG Blocks are found together, it is called an "egg box" (Nagano et.al.,1999). Divalent cations like Calcium (Ca^{2+}) can bind with the G Blocks of adjacent alginate chain thereby crosslinking it. This crosslinking is ionic and leads to gelation of the alginate. The sodium ions are replaced with calcium and the eluted sodium ions combine with the chloride ions of calcium chloride thereby forming sodium chloride and water. When calcium alginate is made to flow in a controlled manner, vertically

downward through sodium alginate solution with more majority of G blocks than M Blocks, then channels are formed. The mechanism of ordered gelation is illustrated in figure 6. Crosslinking by divalent ions hold the monomers in a more structured manner inorder to form the microchannels.

$$Na(Alginate) + CaCl_2 \rightarrow 2\ NaCl + Ca(Alginate) + H_2O$$

The hydrogels so formed were found to be non-toxic and biocompatible with good rate of biodegradability (Yamamoto et. al., 2010).

Mammalian testis is ovoid, reproductive endocrine organs responsible for production of sperm and testosterone. They are suspended in the scrotum by spermatic cord and dartos muscle along with blood vessels. Average testicular dimensions are 4–5 cm in length, 2.5 cm in breadth and 3 cm in anteroposterior diameter; their weight varies from 10.5–14 g in mouse. It contains three layers namely, Tunica vaginalis, Tunica albuginia and Tunica vasculosa.

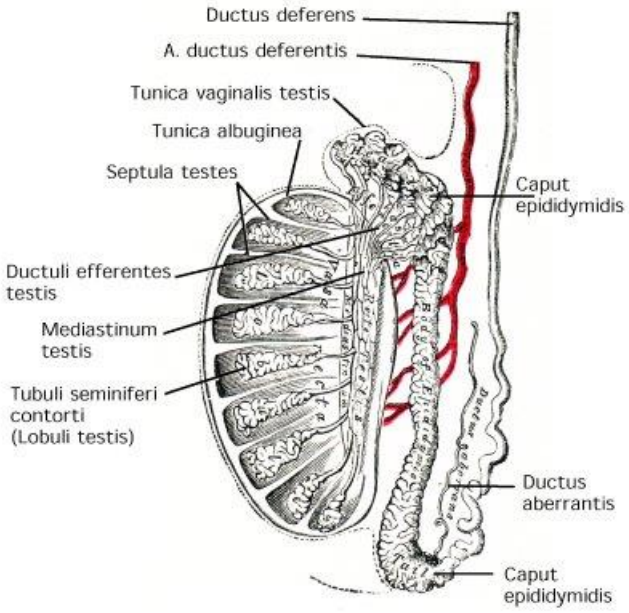

Figure 7: Structure of a Testis (Whillis et.al.,1954).

The testicular lobes contain convoluted seminiferous tubules that are much coiled. Their free ends empty into channels that end in mediastinum. There are 400–600 seminiferous tubules in each testis, each 70– 80 cm long. The diameter of the seminiferous tubules ranges from 0.2 to 0.3 mm. Table 2 shows the diameter of seminiferous tubules measured in six samples in human. It shows an average diameter of 258±27.5 µm with a thickness of 9.9 µm.

Table 2: Diameter of Seminiferous Tubules (Noguera et.al.,1999)

Sample	Diameter of Seminiferous Tubules (µm)	Thickness of Lamina Propria (µm)
1	287.5	9
2	273.7	7
3	206.8	11.5
4	256.6	11.2
5	258.5	13.2
6	265	7.5
Mean	**258.0166667**	**9.9**

The mechanical properties of testis tissue as obtained from various literatures are summarized below:

Table 3: Physical properties of testis

Property		Value	Reference
Density		1082 Kg/m^3	Duck et. al.,2013
Heat Capacity		3778 J/Kg/ºC	Mcintosh et.al..,2010
Thermal Conductivity		0.515 W/m/ºC	Mcintosh et.al..,2010
Heat Transfer Rate		199.81 mC/min/Kg	Mcintosh et.al..,2010
Heat Generation Rate		3.0944 W/Kg	Mcintosh et.al..,2010
Young's Modulus, Border Area	Emean	22.0 ± 5.10 KPa	Sun et. al.,2015
	Emin	18.90 ±4.29 KPa	
	Emax	27.87 ±5.78 KPa	
Young's Modulus, Central Area	Emin	3.97 ± 0.95 KPa	Sun et. al.,2015
	Emax	1.60 ± 0.35 KPa	

Modification of the alginate hydrogel so that it could attain properties similar to those described in Table 3 would make it resemble the physical nature testis. Thus, all these considerations must be given importance while preparing a scaffold for the in vitro self-renewal and differentiation of SSCs.

CHAPTER 3

OBJECTIVES

- To model and simulate the behaviour of mouse SSCs in their Niche.

- To validate the model.

- To design and develop scaffolds for testicular tissue engineering as per the model developed in objective 1.

- To perform physiochemical characterisation of the scaffold developed in objective 3.

CHAPTER 4

MATERIALS AND METHODS

4.1. SIMULATION OF SSC NICHE

4.1.1. SOFTWARE SYSTEM

Matlab, the mathematical analysis software from Mathworks.inc (Matlab Documentation, 2005) was acquired with an institutional license and was used to design the model. No particular toolbox was used to design the model. All the codes were written as basic Matlab 'm' scripts. All the processes were defined as functions to increase the modularity of the code and to reduce the complexity.

Matlab was chosen as the platform for the following reasons since it uses arrays for mathematical manipulation which is exactly what is needed to simulate the concepts put forward in the literature review. It could easily create matrices and manipulate them with lesser code complexity and greater readability. Matlab's Graphical User Interface (GUI) helps us debug the code step by step. During debugging, the variables can be analysed with a few mouse clicks unlike the other programming platforms that do not have such friendly user interface to display variables. Automation of the whole process can be done with loops and pre-defined values for variables. But, changing values of variables in real-time is not possible in Matlab during debugging. The output can be converted into image with *imagesc* function and can be saved to the working directory with the help of *saveas* function. The compiler is user friendly with all possible syntax corrections and probable logic corrections before code execution.

The logics of the developed program are discussed below. The detailed source code is provided in Annexure 1.

4.1.2. STEM CELL NICHE:

The cylindrical seminiferous tubule is modelled as a rectangular area as shown in Figure 8.

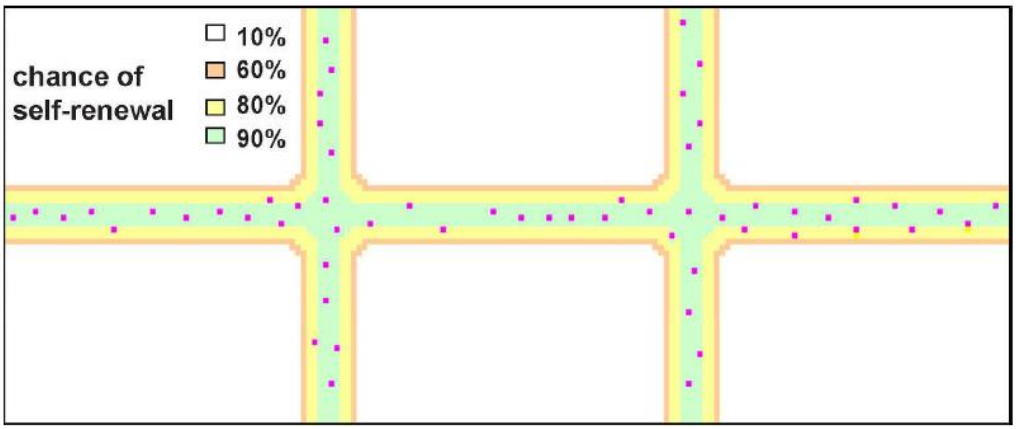

Figure 8: SSC niche as modelled by de Rooij et. al,2012.

The whole rectangular area is the virtual depiction of the circumference of the cylindrical seminiferous tubule. The niche was created as shown in the Figure 9. Thus, the rectangle depicts the basal membrane that houses the spermatogonia A. Every block had a probability from 90% to 10% depending on their distance from the virtual vasculature. The closer the block to the vasculature, higher the probability of self renewal. If the probability of self renewal at a certain area is 90 %, and it contains 10 cells, it means that out of the 10 cells, 9 will self-renew and 1 will differentiate.

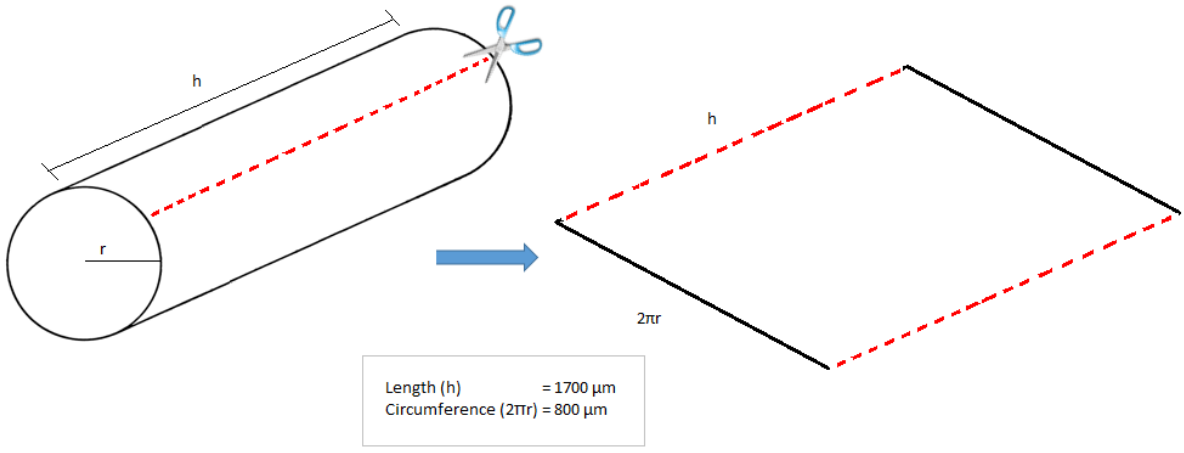

Figure 9: Modelling of Seminiferous Tubule of radius 'r' and height 'h'. The circumference of the cylindrical tubule is modelled as a rectangular area since the A spermatogonia are found only at the circumference of the tubule i.e. Basement membrane

4.1.3. CELL SEEDING

Seeding was done randomly at the niche areas where the probability of self-renewal is 90%. It is not mandatory to seed only at this area. Seeding can be as random as possible and the modularity of the code helps varying the seeding. The number of cells seeded varied from 6 to 20. After seeding, the cells will migrate to reduce contact inhibition. Migration will be according to the cell density which is discussed in section 3.1.4. Such a niche area will contain 4000 sertoli cells as shown by Lok et. al., 1982. An A_s cell is found per 100 Sertoli cells in a niche. Hence, the model is developed such that, after seeding, the A_s cells will repopulate themselves in the niche till their population remains constant at around 45 cells.

4.1.4. CELL DENSITY CALCULATION

The Density Stress effected upon a particular array block by a cell at the position 'i' is given by,

$$D_i = 1/ (d_i)^2$$

(Note: The numerator must actually be the size of the cell 'i'. But, regardless of the cell size, since the cell would occupy only a single block in an array, the size is taken as 1.)

Where,

'D' is the density effected upon the considered array block by the cell 'i'.

'd' is the Euclidean distance between the considered array block and the cell 'i'.

'i' must be a cell that is at most 160µm away from the considered block.

Density stress contributed by all the cells on the considered array block: i.e. Density Contour:

$$D = \sum D_i$$

Thus, a density contour map is created for the whole seminiferous tubule.

(Note: The word density actually refers to the Density factor and not the actual cellular density except if denoted otherwise.)

Let us consider that the density stress on the cell, c_0 in Figure 10 has to be calculated and it is surrounded by 5 other cells in the niche c_1, c_2, c_3, c_4, and c_5. Let c_1, c_2, c_3 and c_4 be at a distance less than 160 µm from c_0 and let c_5 be at a distance greater than 160 µm from c_0.

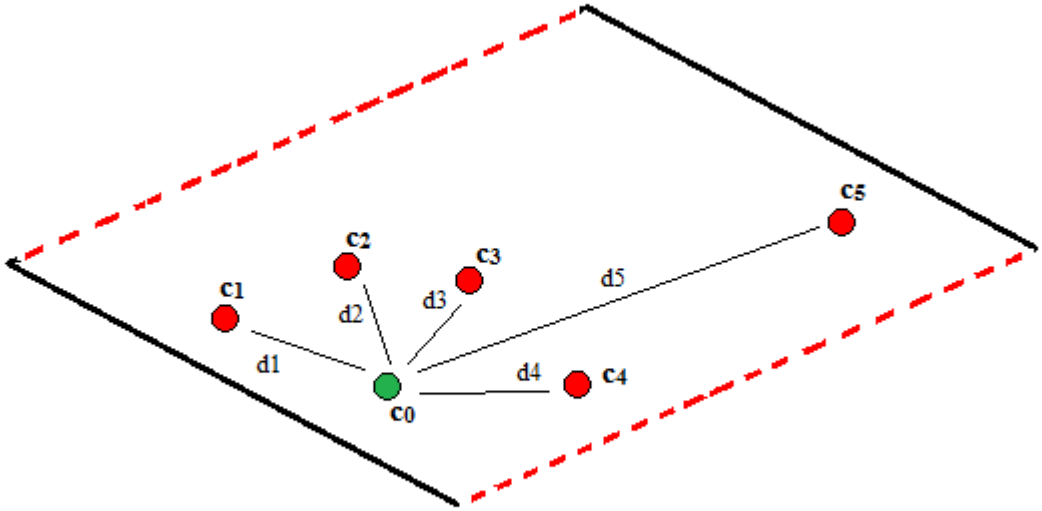

Figure 10: Calculation of the Density Stress on cell c_0 effected upon by the cells c_1, c_2, c_3, c_4 and c_5 which are at a distance of d_1,d_2, d_3, d_4 and d_5 respectively from c_0.

Then, Density Stress on the green cell is calculated by:

$$D = 1/d_1^2 + 1/d_2^2 + 1/d_3^2 + 1/d_4^2$$

Where,

d_1 is the Euclidean distance of c_1 from c_0

d_2 is the Euclidean distance of c_2 from c_0

d_3 is the Euclidean distance of c_3 from c_0

d_4 is the Euclidean distance of c_4 from c_0

d_5 is the Euclidean distance of c_5 from c_0

Since d_5 is at a distance greater than 160µm from the green cell, it does not contribute to density stress.

4.1.5. CELL MIGRATION:

Cell migration happens only when there is a chance of contact inhibition. The cells are less likely to migrate if the density of the block on which it resides is less than the minimum threshold value. If the density is very high above than a maximum threshold on all the surrounding blocks, the cell will not migrate even if its density stress is above than the minimum threshold value. Only A_s cells have the capability to migrate. It was assumed that Apr and Aal cells do not migrate.

Cell migration is inversely proportional to density. Also, It depends on the probability of self-renewal since the As cells tend to remain in the area where the probability of self-renewal is maximum. Migration is the key function that helps the cells surpass contact inhibition. Contact inhibition occurs at mammalian cells when they are as close as 40 µm thereby, not letting them divide. So, if the cells don't migrate, there will be local clumping of cells in the niche that will prevent their division and thereby affecting the steady state of the niche.

Since the cylindrical seminiferous tubule is modelled in a rectangle, the cells that are lost through the upper portion of the niche during migration will re-emerge through the lower portion of the niche as shown in Figure 11.

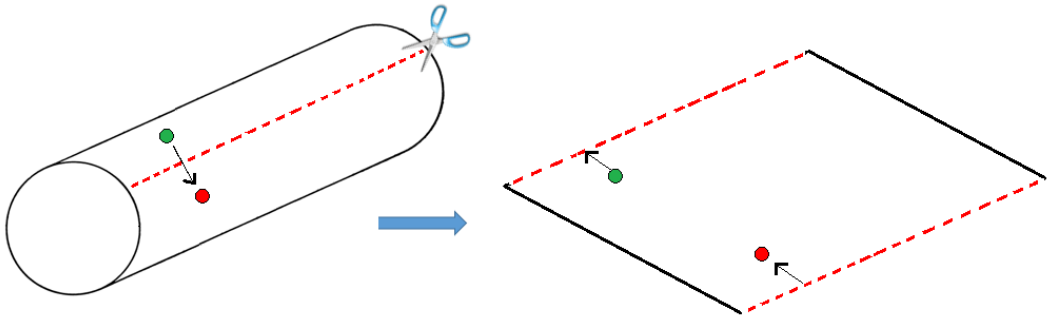

Figure 11: Modelling of Cylindrical Tubule in a Rectangular area

If the green cell moves to the position of red cell in the seminiferous tubule, it is modelled in the rectangular niche such that instead of getting lost through the edges, the red cell re-emerges from the opposite end. Thus the continuity of tubule is maintained.

4.1.6. SELF RENEWAL AND DIFFERENTIATION:

Self-renewal occurs preferentially when the cells are at a distance of at least 40 µm from each other or otherwise it will lead to contact inhibition (Jing et.al.,2009). Since self-renewal is not synchronised in A_s cell population, they will divide at random. After self-renewal, the A_s cells will give rise to a daughter cell only if the daughter cell has space to move away from the parent As cell. The distance it should move away from the parent can be any but greater than 25 µm. The maximum distance that a daughter cell can migrate is set to either 60 µm or 80 µm depending on the steady state conditions. The A_s cells are sorted in ascending order of their density stress during self-renewal. The daughter cells of the cells that are in the first half of the sort order migrate to 80 µm and the daughter cells of the next half of the sort order migrate to 60 µm from each other. The decision whether the cell has to self-renew or differentiate depends on the probability of self-renewal defined in the niche which is co-related to vasculature. If the probability of self-renewal is 90% in an area, then, 9 cells out of 10 self-renew and one cell differentiates into Apr.

Cell division is segregated into cycles. Each cycle has three divisions in it. In the first two cycles, all the A_s cells divide. In the third cycle, only a percentage of cells divide in order to maintain the number of cells in the niche. If an A_s cell is set for differentiation, then, its size becomes doubled in an array block. Differentiation is a synchronous process and hence all cells set to differentiate will differentiate at the same time. A_s cells will differentiate into Apr cells, Apr cells will differentiate into A_{al4} cells, A_{al4} cells will differentiate into A_{al8} cells and A_{al8} cells will differentiate into A_{al16} cells. A_{al16} cells will not differentiate further till harvest since A_{al32} cells are not common in rodents.

4.1.7. CELL HARVEST:

After the third division of an epithelial cycle, the cells are harvested. This depicts the stage VII/VIII of the epithelial cycle where the A spermatogonia differentiate into A_1 spermatogonia and leave the basal membrane so that it could reach the lumen as a spermatocyte. Almost all of the A_{al8} and A_{al16} cells are harvested and half the A_{al4} cells are harvested. After harvesting, the cells again are directed to the first division of the next cycle.

4.2. PREPARATION OF MICROTUBULAR SCAFFOLDS

All chemicals are procured from HiMedia Laboratories private limited (Mumbai, India), unless otherwise specifically indicated.

4.2.1. PREPARATION OF SODIUM ALGINATE SOLUTION:

0.5%, 0.75%, 1% and 2% w/v sodium alginate solutions in distilled water were prepared. Sodium alginate (Molecular Biology Grade) was weighed accordingly and was slowly dissolved in a beaker with distilled water while kept in a magnetic stirrer at 300 rpm. It is recommended to dissolve the sodium alginate Initially with half the volume of distilled water and then the remaining volume of water was added to prevent clogging of sodium alginate at the center of the beaker. The solution was stirred for at least 8 hours at room temperature.

4.2.2. PREPARATION OF CALCIUM CHLORIDE SOLUTION:

0.5M, 1M 1.5M and 2M Calcium Chloride dihydrate ($CaCl_2.2H_2O$) solutions were prepared to the required volume by dissolving it in de-ionised water. Calcium Chloride was weighed accordingly and slowly dissolved in distilled water while stirring at 250 rpm. Calcium Chloride exothermically reacts with water thereby releasing heat and therefore, the beaker's mouth was closed with an aluminum foil to prevent evaporation of water. The solution was stirred for at least 1 hour at room temperature.

4.2.3. PREPARATION OF GELATION MOULDS:

100 mL beakers were used as gelation molds. The beakers were initially coated with sodium alginate solution and were dried in hot air oven at 80˚C for 15 minutes. Two to three such coatings are done in order to prevent the alginate gel from sticking to the walls of the beaker after gelation.

4.2.4. PREPARATION OF HYDROGEL:

20 mL of the prepared sodium alginate solution was taken in the alginate coated mold. A thin layer of $CaCl_2$ solution is then gently sprayed over the alginate solution. Thus, only a thin layer of $CaCl_2$ (less than 1mm thick) is allowed to react with sodium alginate to form a single layer of gel called primary layer. After the formation of primary layer, 10 mL $CaCl_2$ solution is gently added over the primary layer. The whole setup was kept undisturbed for 18–24 h. After gelation is complete, the gel was removed from the mould and was cut into small pieces of 1cm x 1cm x 2cm along the capillary axis. These pieces were then immersed in distilled water and was kept in an orbital shaker for at least 24 h in order to remove excess $CaCl_2$ and the formed NaCl. The gels were stored in distilled water or 30% ethanol at 4˚C until analysis.

4.2.5. CHARACTERISATION OF SCAFFOLDS:

To analyse the pore and channel morphology, microscopic studies were carried out.

i. OPTICAL MICROSCOPY:

After anisotropic gelation of alginate, and the removal of excess Calcium Chloride by exchange with distilled water, the gels were subjected to microscopic studies. The gels were cut with No.11 Bard Parker™ Blades along the capillary axis to visualize the channels and perpendicular to the capillary axis to visualize the pores. The images were taken with a Carl Zeiss Microscope.

ii. SCANNING ELECTRON MICROSCOPY (SEM)

To visualise the gels in SEM, they had to be dried. Since the scaffolds were made with 0.5 %, 0.6% and 0.75% Alginate solutions, they were too fragile to withstand the freezing before freeze drying. Hence, the gels were cut into thin sections and then were fixed in 2.5% electron microscopy grade glutaraldehyde solution for about 4 hours. Longer the time, better was the fixation. After fixation, the gel was dried in an ethanol gradient. 30%, 40%, 50%, 70%, 90% and 100% ethanol were prepared and the gel was immersed in each in order for about 20 minutes. After 100% ethanol treatment, the gel was dried under vacuum. The dried gel was kept on stubs, coated with Gold (Au) and Platinum (Pt). They were then analysed in NanoSEM™ under vacuum at a voltage of either 5kV or 10kV and a magnification of 100x to 500x.

4.2.6. PHYSIOCHEMICAL CHARACTERISATION

i. SWELLING STUDY:

The calcium alginate gels were dried in ethanol gradient as described in section 4.25 but without glutaraldehyde fixation. The dried gel samples were then taken in 10mL beakers and were immersed in 3 mL of autoclave Phosphate buffered saline. For every hour, the sample was taken out of PBS, blotted in Kimwipes^{TM} (Kimberly Clark Corp.) and were weighed. The process was carried out till the scaffolds stopped swelling or till they degraded in PBS. The swelling percentage was calculated with the formula,

$$\% \text{ Swelling} = [(W_t - W_0)/W_0] * 100$$

Where,

W_0 is the initial weight

W_t is the weight at time 't'

A graph was plotted between time and the swelling ratio.

ii. FOURIER TRANSFORM INFRARED SPECTROSCOPY (FTIR)

Fourier Transform Infrared Spectroscopy (FTIR) was used to study the interaction of compounds in a sample. The gel sample was air dried and then powdered using mortar and pestle. The powdered sample was then ground along with Potassium Bromate (KBr) and was made into a pellet. The pellet was then analyzed by FTIR to know the interaction between various bonds.

iii. MECHANICAL ANALYSIS

Compression testing was done with the help of Texture pro CT Texture Analyser (Brookfield Engineering Labs. Inc.). A 4 mm TA44 cylindrical probe was used to compress the samples at a speed of 0.1 – 0.5 mm/s. The trigger load was set to 0.1 N so that the surface of the sample is not damaged before experimentation. The distance of compression was fixed to 3 mm and the force required to compress the samples to 3 mm was determined.

CHAPTER 5

RESULTS AND DISCUSSION

5.1. SIMULATION OF SSC NICHE

5.1.1. SSC Niche

The SSC Niche was created according to the pattern of blood vessels shown by Yoshida et al.,2007 The niche is as shown in Figure 12. It contained areas of self-renewal with probability values 90%, 80%, 60% and 10%. One out of every ten cells in the 90% probability area differentiates whereas one out of every 10 cells in the 10% probability area self-renew. It is believed that SSCs are present mostly in the areas where blood vessels branch. Hence, the niche probability is created in relation to the path of blood vessels in the 3D reconstruction of SSC niche by *S*hetty et. al.,2007.

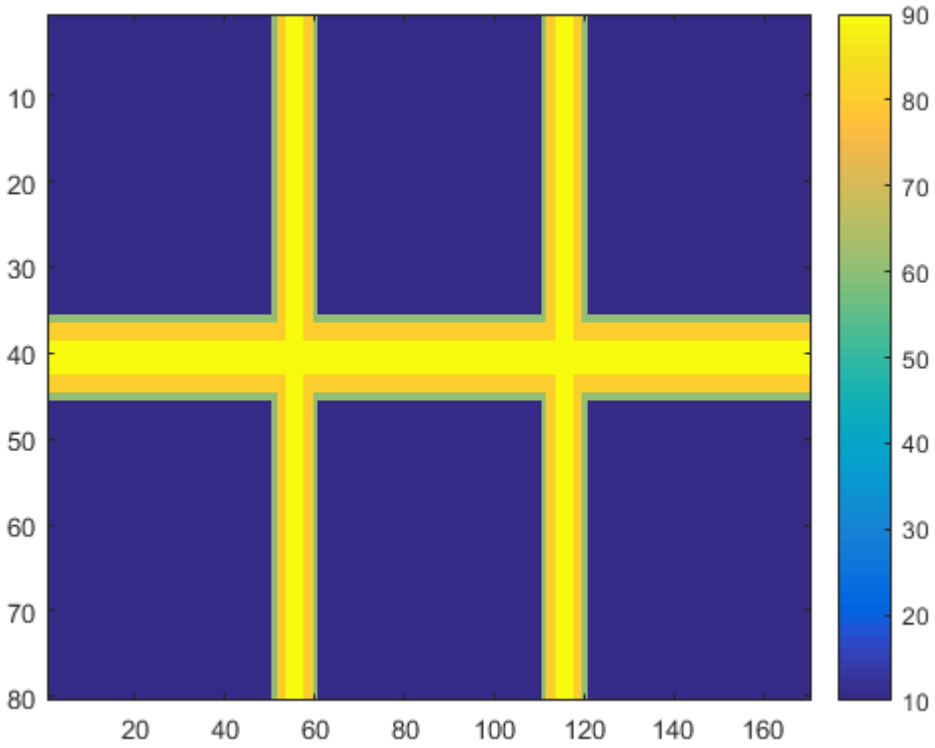

Figure 12: SSC Niche with different probability of self-renewal as simulated by Matlab

Seeding was done initially in the area where probability of self-renewal is 90%. All the SSCs seeded were A_s cells. Every time the program is run, SSCs are seeded differently.

This was achieved by using the random number generators in Matlab. So, the precision of randomising the process depended only on the trustworthiness of the Random number generator in Matlab. A custom probability density function could be used to generate custom random numbers that could make the randomisation more robust. The cells were seeded as shown in Figure 13. The seeded array shown in Figure 13 was used for all the following results generated unless mentioned otherwise. The number of cells seeded could be controlled by adjusting the seeding factor.

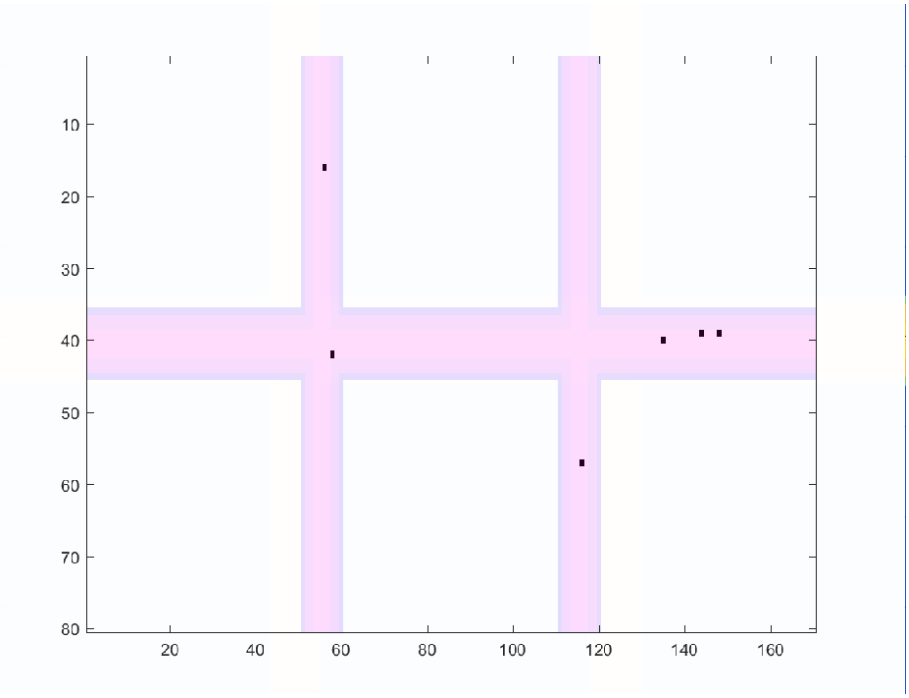

Figure 13: Cell seeding in the niche. Randomly, 6 Cells were seeded in the 90% probability area.

After seeding, the SSCs started migrating so as to avoid contact inhibition. The threshold for contact inhibition is 40 μm. It can be chosen manually. Subsequently after migration, the stem cells divided. If the number of A_s cells was less than 40, the stem cells only self-renewed. This was to repopulate the niche. This could be visualised to be the situation that arises when the niche has been damaged (e.g. By irradiation). After repopulation was done, the further divisions accompanied differentiation of the cells according to the area they are in. The migration of the cells was such that they will preferred to stay inside the niche in an area where the probability of self-renewal was higher. Hence only under extreme density conditions, they migrated out of the niche. This threshold could also be given manually.

After a number of divisions, steady state formed which resulted in a constant number of A_s spermatogonia and appropriately steady rate of production of A_{pr} and A_{al} spermatogonia. This steady state depended mostly on the number of A_s cells, the probability of self-renewal and the density thresholds within which the stem cells migrated and divided. The number of A_s cells and the probability of self-renewal were given as inputs along with the niche and seeding. Hence, the only controllable variable was the density thresholds within which the cell would migrate and divide.

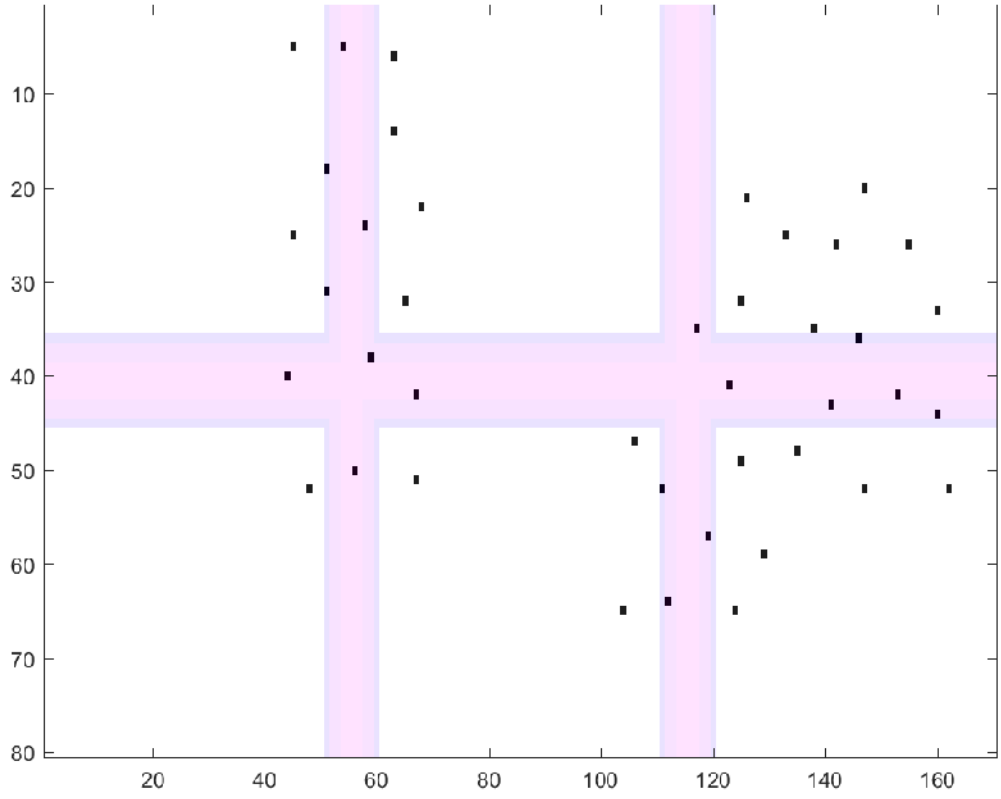

Figure 14: Repopulating stem cells in the niche after seeding. Repopulation was carried out for either 6 divisions or until the niche has at least 40 As cells.

After repopulation, the stem cells entered the normal epithelial cycle. An epithelial cycle involved 3 divisions. The cells divided randomly and within a cycle of seminiferous epithelium, a cell divided at least 2 times. Simultaneously, some cells entered the differentiation pathway in-order to produce A_{pr}, A_{al} and simultaneously A_1 spermatogonia. This kinetics depended on the density.

5.1.2. CELL DENSITY:

Cell density was calculated by the below formula,

$$D_i = 1/(d_i)^2$$

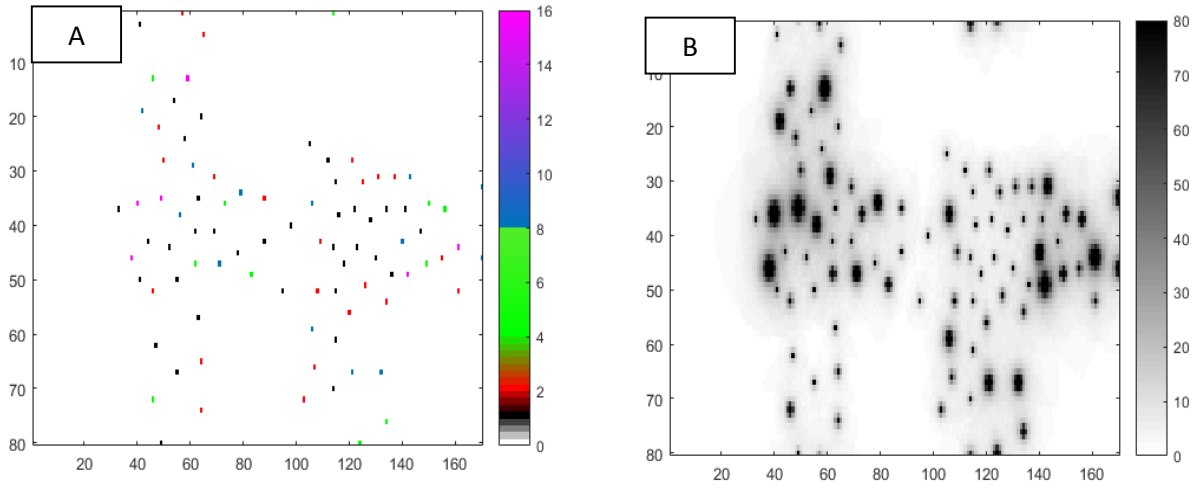

Figure 15: A density contour map. **A:** The cell distribution in the niche **B:** Density contour map for the cell distribution shown in A.

A contour map is created with the density stress on each block because of the surrounding cells. In the contour map (Figure 15 B), the darkest patches are high density areas, where, the density stress is very high and the lighter patches are blocks where, the density stress is very less. By manipulation of density contour map, the migration, division and differentiation of a cell is controlled by various thresholds.

5.1.3. CELL MIGRATION:

Cell migration happened only when there was a chance of contact inhibition. Contact inhibition occurred when the distance between the cells was less than 40 µm. The function for migration was stated such that the cell which resided on the array block that had the highest density influence migrated first. Migration was done block by block and with the cell moving to the block with the least density stress. If the neighboring blocks were at a density stress higher than that of the cell's position, the cell did not migrate. Conversely, if the cell was at a position where the density stress was less than the threshold, the cell did not migrate.

5.1.4. CELL DIVISION AND DIFFERENTIATION:

Cell division was segregated into cycles. Each cycle had three divisions in it. In the first two cycles, all the cells divided. In the third cycle, only a percentage of cells divided in order to maintain the number of cells in the niche. If an A_s cell was committed for differentiation, then, its size becomes doubled in an array block. Differentiation was a synchronous process and hence all cells committed to differentiate differentiated at the same time.

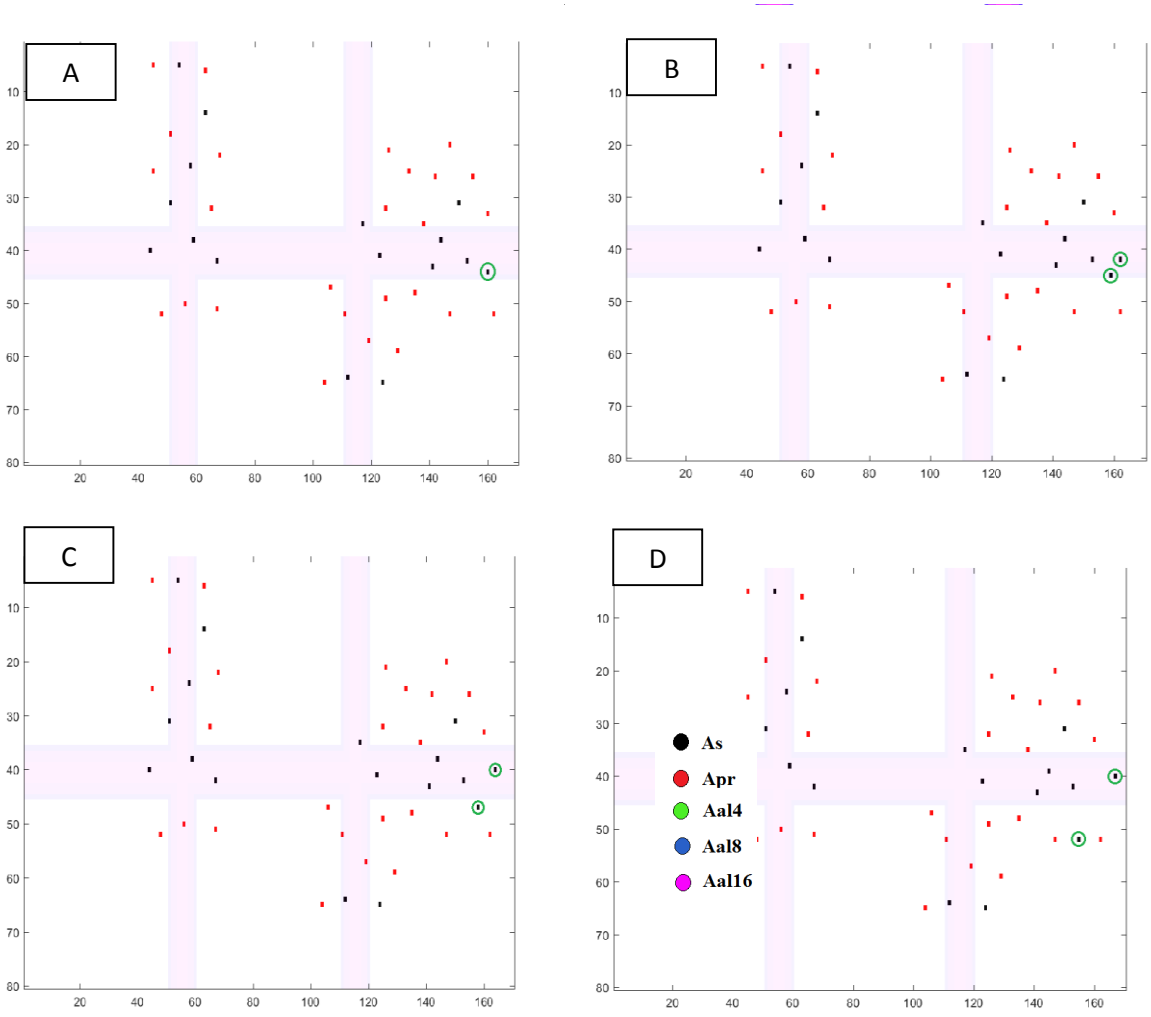

Figure 16: Schematic of cell division. A: As cell (Circled) is committed for self-renewal. B: The committed cell divided and two daughter cells are formed. C: The Daughter cells started to migrate D: The daughter cells migrated. One daughter stays inside the niche and the other goes out to be differentiated

Figure 16 shows division and migration of A_s cells. A_s cells divided randomly. After an SSC is committed for self-renewal, it checked the surrounding space for any density stress. A density threshold was set such that the SSC will not divide if it is in a density stress higher than that of the threshold. If the density stress on the SSC was lower than the threshold, it meant that, if the SSC divided, then the daughter cells would have enough space to migrate away from each other in order to avoid contact inhibition. The SSC committed for self-renewal divided and the daughter cells occupied two new blocks (Figure 16 B). After division, they started to migrate away block by block. Most of the times, it was such that one of the daughter cell would stay inside the niche and the other would migrate away from the niche. (Figure 16 D). This was to maintain the steady state of the niche.

Differentiation was synchronous such that all the cells committed for differentiation differentiated at the same time (Figure 17). In a single division cycle, randomly, one half of the total population of A_s cells was committed to self-renewal and the other half was committed to differentiation. It took 5 division cycles for an A_s cell to become A_{al16} cell which then differentiated into A_1 spermatogonia in the 6^{th} cycle and left the niche (Figure 17F). This process, where, the A_1 spermatogonia left the niche was termed harvest. The cells committed to differentiation never migrated since they were assumed not to move along the lateral direction in the seminiferous tubule, but, still, they contributed to density stress as all other cells. At the same time an A_s cell started to differentiate in an epithelial cycle, there were A_{pr} and A_{al14} cells present from the previous epithelial cycle. It is only from that A_{pr} and $A_{al4,}$ A_{al16} cells were derived in the current epithelial cycle. Hence, at the end of a single epithelial cycle, there were cells from two generations. A_s, A_{al8} and A_{al16} from the previous generation and $A_{s,}$ A_{pr}, A_{al4} and A_{al18} from current generation. The density thresholds for division and process of randomisation are shown in Annexure 1.

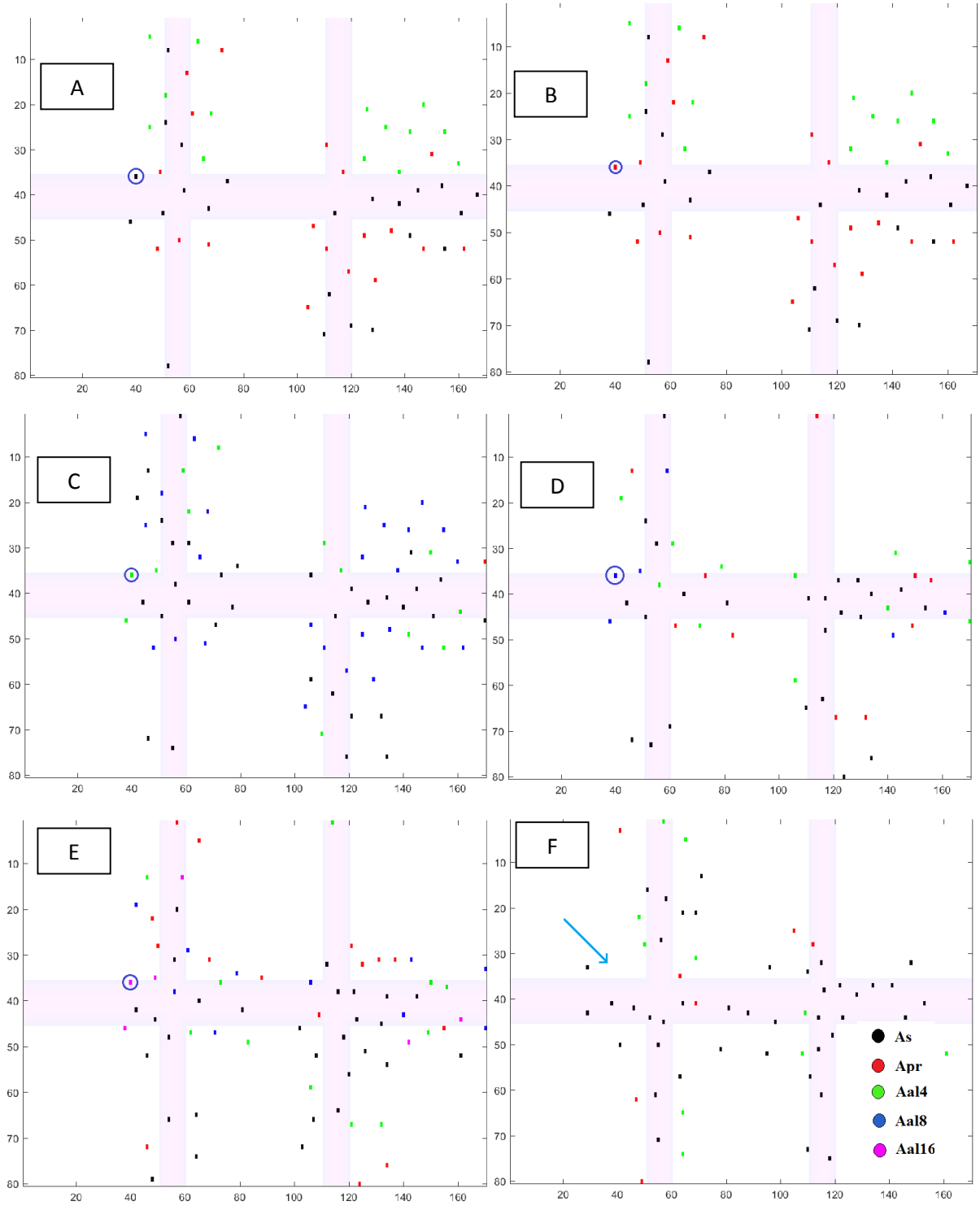

Figure 17: Schematics of cell differentiation. The A_s cell (A) differentiates into A_{pr}(B). A_{pr} becomes A_{al4}(C). A_{al4} becomes A_{al8}(D) and A_{l8} becomes A_{al16}(E). After this, during the harvest stage, A_{al16} is Harvested and the cell leaves the niche(Shown by an arrow in F)

5.1.5. CELL HARVEST:

After the third division of an epithelial cycle, the cells were harvested. This was similar to stage VII/VIII of the epithelial cycle where the A spermatogonia differentiated into A1 spermatogonia and left the basal membrane so that it could reach the lumen as a spermatocyte. Almost all of the A_{al8} and A_{al16} cells and half the A_{al4} cells are harvested. After harvesting, the cells were redirected to the first division of the next cycle.

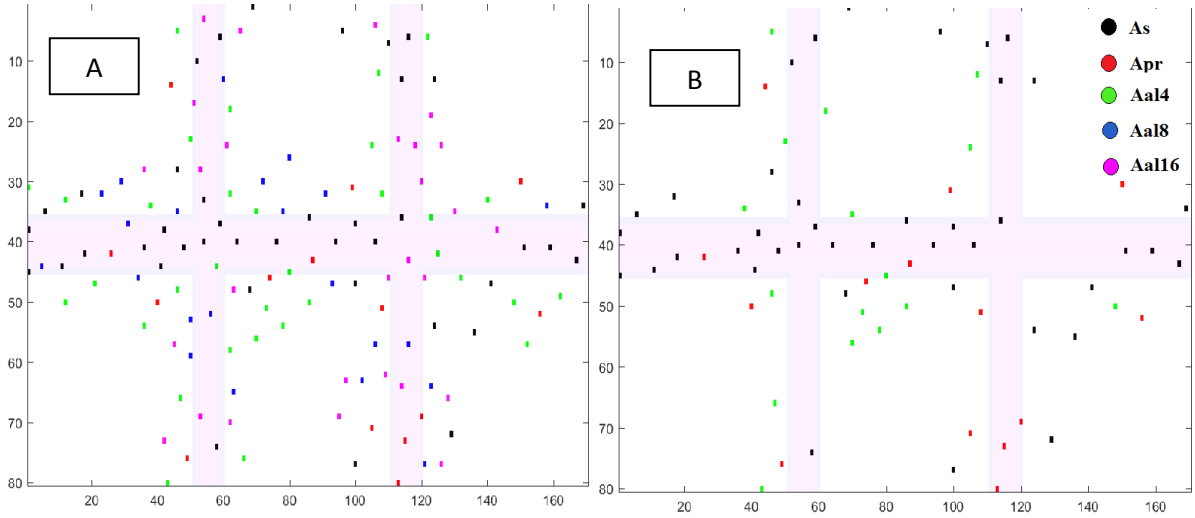

Figure 18: Schematic of cell harvest (Differentiation into A_1 Spermatogonia). Half of A_{al4} cells and all the A_{al8} and A_{al16} cells were harvested. **A:** Before harvest. **B:** After harvest.

Figure 18 shows the harvest phase of an epithelial cycle. Figure 18A is the state of the niche before harvest. It can be found that there were totally 140 cells in the niche before harvest and there are only 69 cells in the niche after harvest. 71 cells were harvested out of which there were 22 A_{al8} cells, 23 A_{al4} cells and 26 A_{al16} cells. The number of cells harvested at the end of each epithelial cycle varied considerably. The number of cells harvested was found to be 61±7 out of which there were 15.15±2 A_{al4} cells, 16.71 ±4 A_{al8} cells and 29.04 ±4.9 A_{al16} cells. It was found that A_{al16} cells contribute more to the population of A_1 spermatogonia than that of A_{al4} and A_{al8} cells. In a single epithelial cycle, two A_{al16} cells differentiate into A1 spermatogonia per A_{al4} and A_{al8} cell.

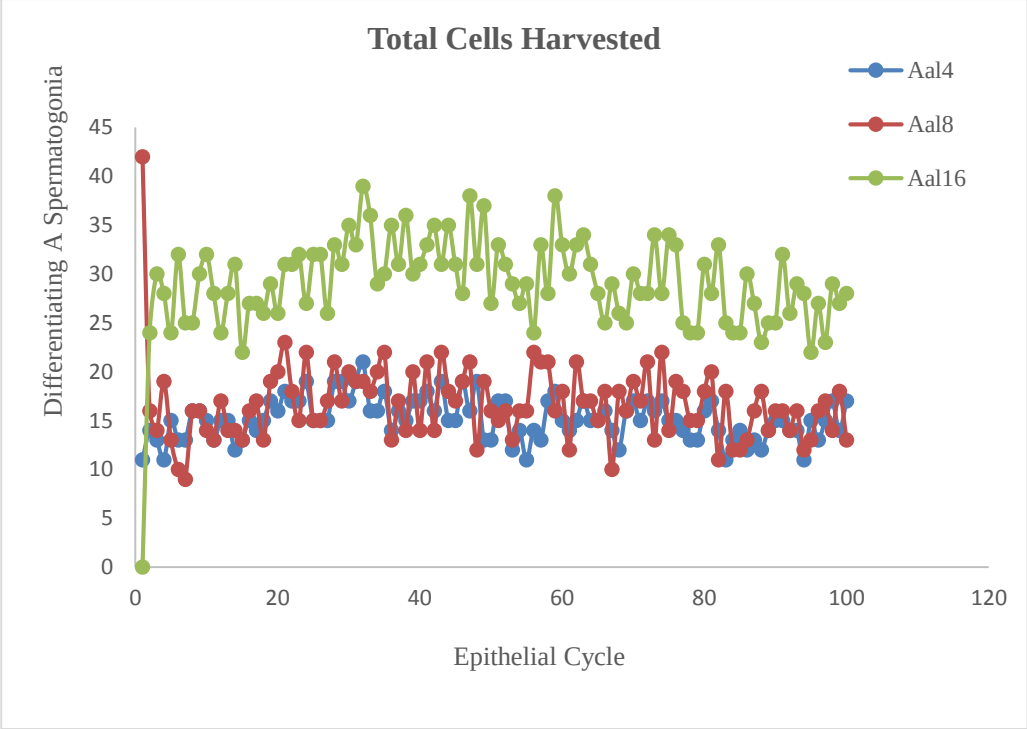

Figure 19: Harvest results for 100 epithelial cycles. Though the cell number is not always steady, it stays around a mean value of 61 cells.

5.1.6. CELL COUNT:

Since the whole program was simulated with randomness in consideration, the cell counts varied considerably between the cycles. The number of A_s spermatogonia was 45.92±5.75 as shown in Figure 20.

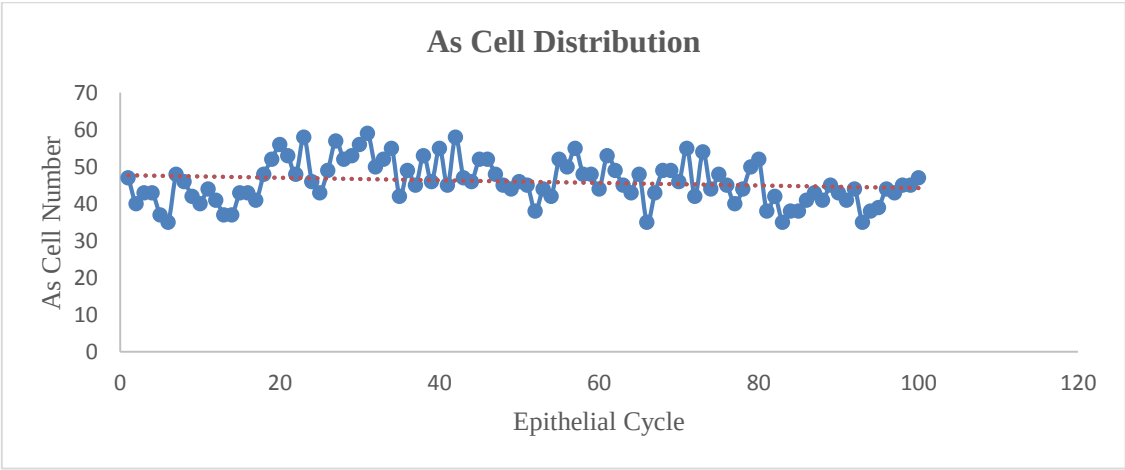

Figure 20: Count of number of A_s Spermatogonia. Mean Cell no. = 45.9 cells/ cycle

The distribution of A_s spermatogonia is each division of an epithelial cycle was determined. It was found that the count of A_s spermatogonia was higher in the second division of the epithelial cycle with 56.7±6.8 cells. It was fairly equal in the first and second divisions with 46.1± 6.06 and 45.92± 5.76 cells respectively (Figure 21). Thus, it inferred that the program controlled the limit of A_s spermatogonia in the 3rd division of the epithelial cycle and it depended on the density thresholds.

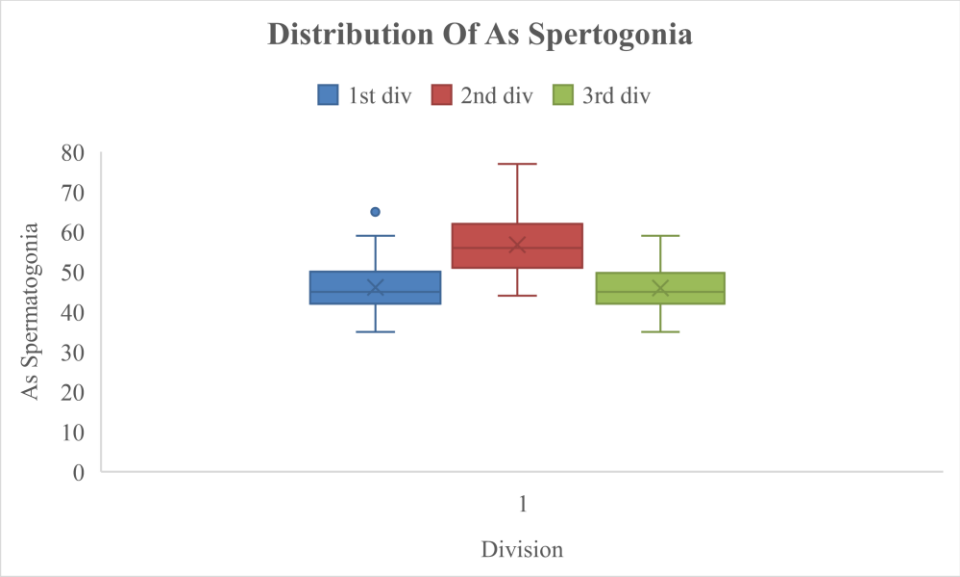

Figure 21: Variation of A_s spermatogonia in the 1st, 2nd and 3rd divisions of epithelial cycle

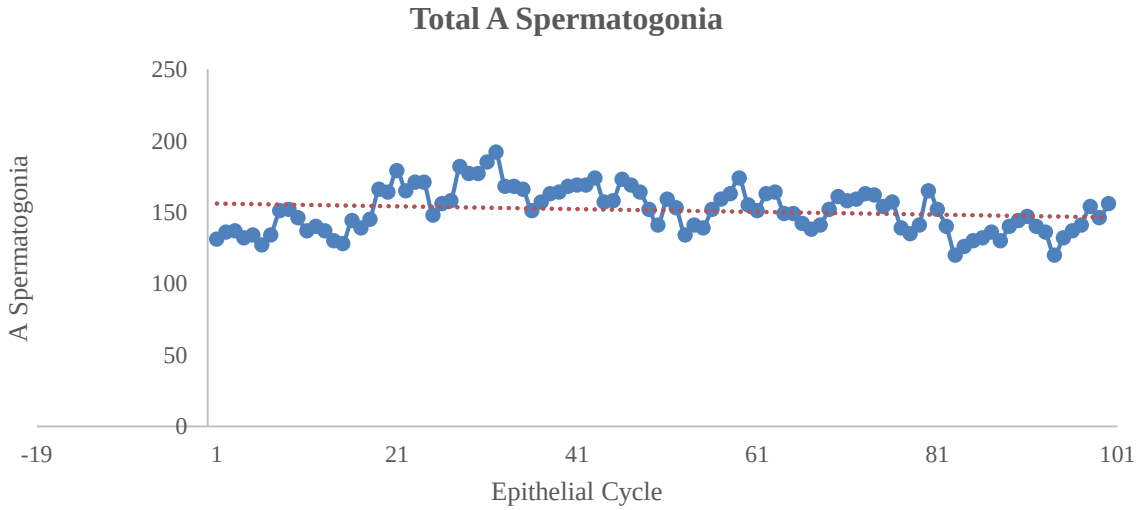

Figure 22: Total A spermatogonia count ($A_s + A_{pr} + A_{al4} + A_{al8} + A_{al16}$) in the Virtual Seminiferous tubule for 100 epithelial cycles. Mean cell no. = 151.33.

There was cycle to cycle variation in the count of total A spermatogonia. The total stem cells varied from 125 to 190. But, because of density regulation in the niche, the total number of spermatogonia fairly remained constant at around 151 cells. The total number of cells depended on density thresholds and on extending the thresholds, such that the cells are allowed to move till a distance of less than 40µm, the number of cells increased. If the threshold window is chosen such that contact inhibition occurred at as high as 80µm, the number of cells drastically decreased and finally, the cells were washed off the niche. Trials like these were done, and the density thresholds were chosen according to the count of spermatogonia obtained in each trial. The thresholds are provided in the code (Annexure 1).

5.1.7. VALIDATION OF THE MODEL:

The developed model was validated against published literature. *Lok et. al.*,1982 counted the number of A spermatogonia available in a rodent per 1000 Sertoli cells. The results of cell numbers obtained by the simulation were found comparable to the results of real counts of A Spermatogonia in rodents.

Table 4: Comparison between the no. of A_s, A_{pr} and A_{al} spermatogonia generated in the developed model and the number found in real count of seminiferous tubule whole mounts for a niche area of 800 x 1700 µm (Lok et.al.,1982).

Cell Counts	**A_s**	**A_{pr}**	**A_{al4}**	**A_{al8}**	**A_{al16}**	**Total Cells**
Real Count	48	32	26	20	26	152
Program Count	45.92	29.83	29	16.71	29.04	151.33

Thus, the above simulation was validated against a literature data and is found to be acceptable. The population of A Spermatogonia could be either increased or decreased by controlling various factors in the code as discussed in chapter 3. By controlling these factors, the density regulation could be controlled thereby managing the niche. Unfortunately, owing to lack of quantitative data in literature, further analysis could not be done. Nevertheless, the qualitative modelling was similar to as expected.

5.2. SYNTHESIS OF CALCIUM ALGINATE GELS

Prior to synthesis of anisotropic gels with calcium chloride, preliminary trials were made to synthesize the gel with 0.5M Copper Sulphate Pentahydrate (data not shown) and 1 – 2% Sodium alginate (Molecular Biology Grade). The Cu-Alginate gels formed were better in terms of pore and channel morphology and also had better strength when compared to Calcuim Alginate gels. But, the maximum channel diameter obtained in a Cu-Alginate gel was not more than 80µm. Hence, they were not suitable for growth of SSCs which require more than 80 µm to grow. If the gel has to mimic the structure of seminiferous tubules, then the diameter should be at least 180µm. Hence, a combination of various salts like NaCl was tried along with Copper Sulphate Pentahydrate, but, it resulted in shrinking of the channels rather than expanding it. It might be because of the competition of sodium and copper for alginate which resulted in shrunken channels. Hence, Calcium Chloride Dihydrate was chosen as the crosslinker instead of Copper Sulphate Pentahydrate. Unlike Copper Sulphate, 0.5M Calcium Chloride did not form any channels with 2% Sodium alginate solution. But, on decreasing the Sodium alginate below 1.5 % and increasing the CaCl2.2H2O concentration to 1 M, channel like morphologies were found and the channels became prominent at Sodium alginate concentrations below 1%. The sodium alginate concentration was lowered below 1% and the gelation was successful till 0.5% sodium alginate solution. Beyond it, the gel was very soft and was very difficult to handle. Calcium Chloride Dihydrate concentrations were also varied and was found that the channels were formed at almost all concentrations of CaCl2.2H2O above 1M. The channel diameter remained constant; only the depth of penetration of calcium chloride in the alginate and rate of formation of gel varied. At increasing Calcium Chloride concentrations, the gelation was faster and it took only 12 h to form the gel with 2M CaCl2 whereas it took 18-24 h for complete gelation with 1M CaCl2.

Hence, 1M CaCl2.2H2O was chosen as the cross linker and the concentrations of sodium alginate was varied from 0.5% to 1% throughout the analysis.

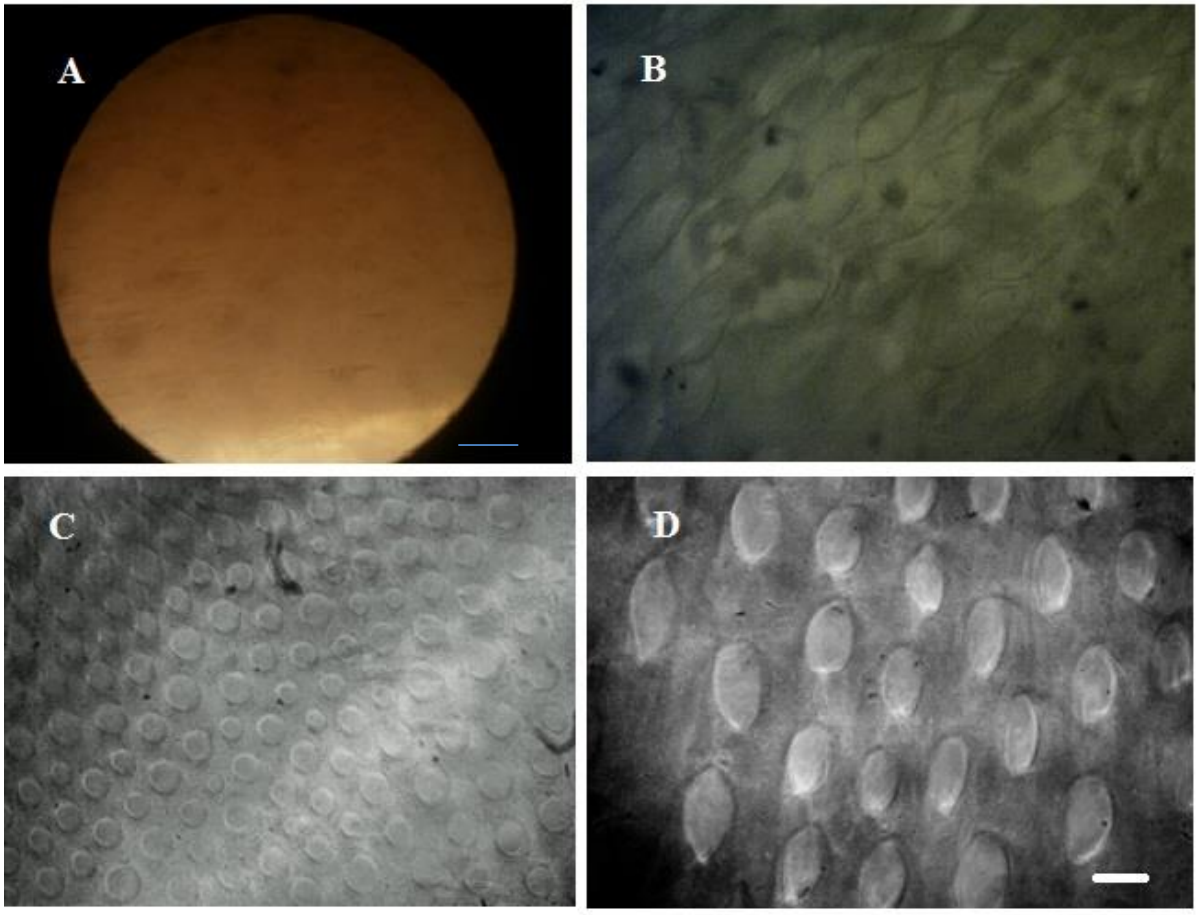

Figure 23: Initiation of pore formation in calcium alginate gels of various alginate concentrations. **A:** 2% Alginate. **B:** 1.5% Alginate **C:** 0.75% Alginate **D:** 0.5% Alginate.
Scale of B, C and D is 100 µm. Scale of A is 200 µm.

5.2.1. SCAFFOLD CHARACTERISATION

i. OPTICAL MICROSCOPY

The calcium alginate gels were cut with No. 24 BP blades and this resulted in damage to the gel. Hence, No. 11 BP blades were used while cutting the gels. The calcium alginate gels did not have a uniform channel diameter. The diameter was the least near the primary layer and was the highest at the bottom of the gel as shown in Figure 24. The diameter of the channels increased with decreasing alginate concentration as shown in Figure 25. Calcium chloride concentration did not seem to affect the diameter of the channels, but with increasing concentrations of calcium chloride the pore geometry became better.

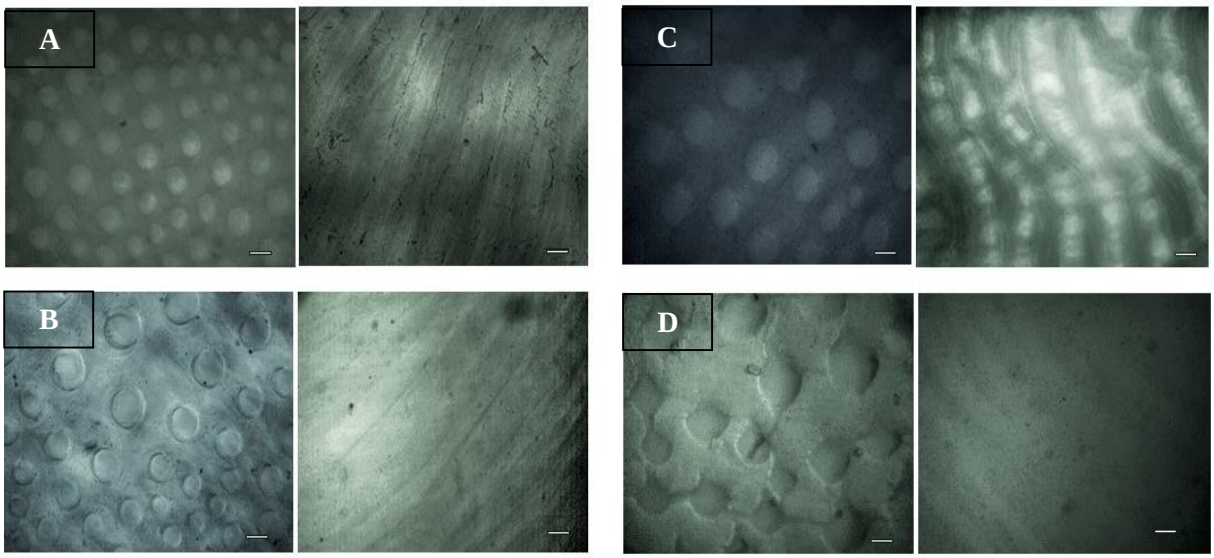

Figure 24: Ionotropic gel produced with 0.75% sodium alginate and 2M $CaCl_2$ and sectioned horizontally and vertically to show channels and pores. The pore size increases with depth. **A**: Near the primary layer, mean diameter = 83.8 µm. **B:** 5 mm from primary layer, mean diameter = 107.5 µm **C:** 10 mm from primary layer mean diameter = 120.004 µm **D:** 20 mm from primary layer, mean diameter = 125 µm. Scale is 100 µm

Though channels were formed in all groups, the repeatability of the process was very poor. The channel diameters varied large extent when casting the gel each and every time for the same concentrations of calcium chloride and sodium alginate. This was because, 10 mL beakers were used as moulds and they were immersed in 100 mL beakers containing CaCl2 after the formation of primary layer. The distribution of calcium ions in such conditions was not even, since the solution in the top portion of the 100 mL beaker would exchange more calcium ions with the alginate solution in the mould than the solution in the bottom of the beaker. This lead to uneven distribution of Calcium ions in the solution due to which there was always a bias in diameter of pores in the gel. Hence, the mould was changed. The alginate solution was taken in a 100 mL beaker and, in the same beaker, calcium chloride solution was sprayed to form the primary layer and then, CaCl2 solution was poured in the same beaker which initiated the formation of secondary gelation layer.

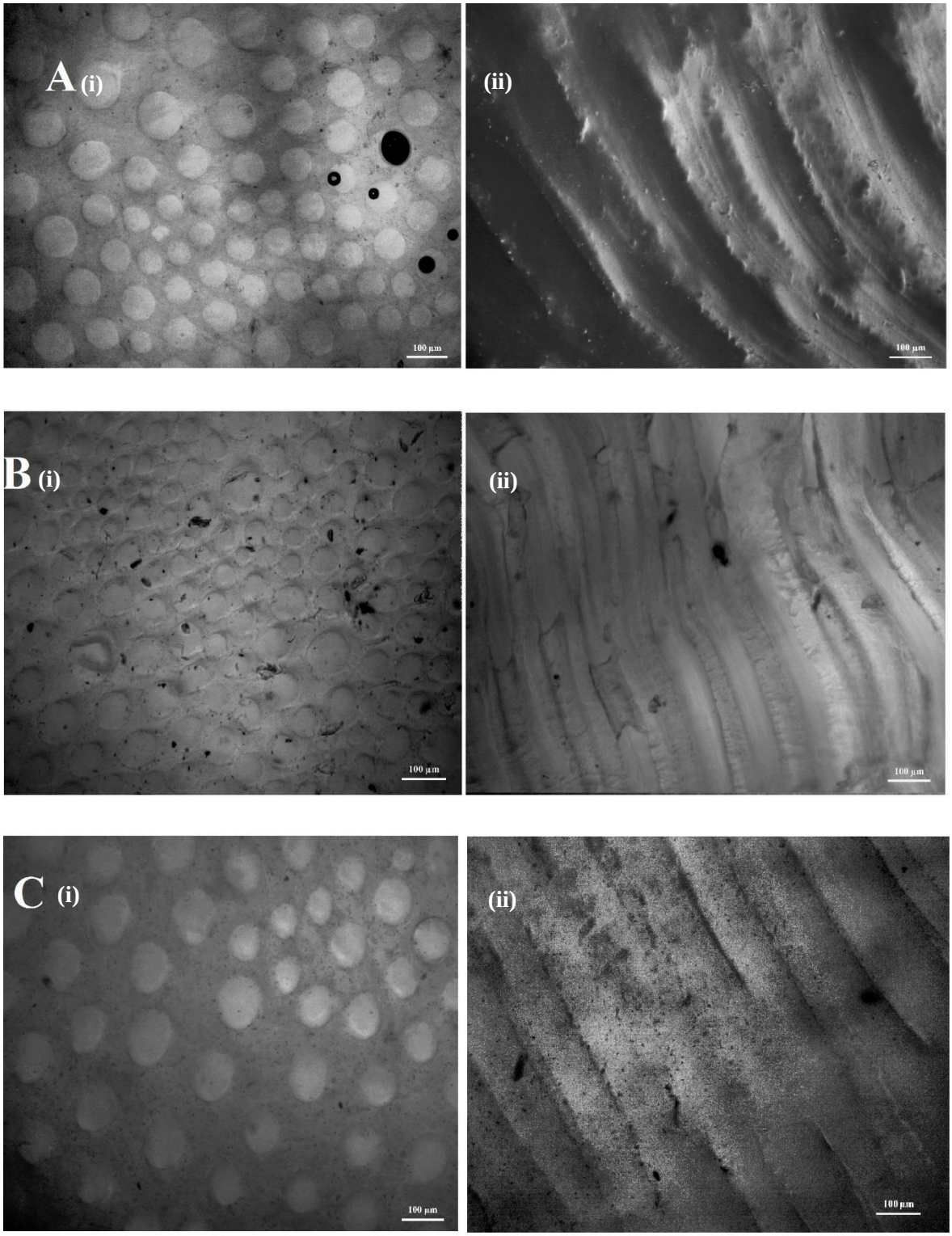

Figure 25: Pore and channel morphologies of gels. **A:**0.5% Alginate, mean diameter = 115 µm **B:** 0.6% Alginate, mean diameter = 90 µm **C:** 0.75% Alginate, mean diameter = 95 µm. Scale = 100µm

After this modification, the gelation was found to be uniform and repeatability was better. There were two types of channels observed. There were channels with uniform diameter and there were well defined tubular structures with more uniformity and prominence. These channels were of a larger diameter and were found equally spaced in the gel. A tubule was at least 0.5 mm away from a similar nearby tubule. These tubules were visible to the naked eye unlike the weaker tubules that had a lesser diameter as shown in Figure 26.

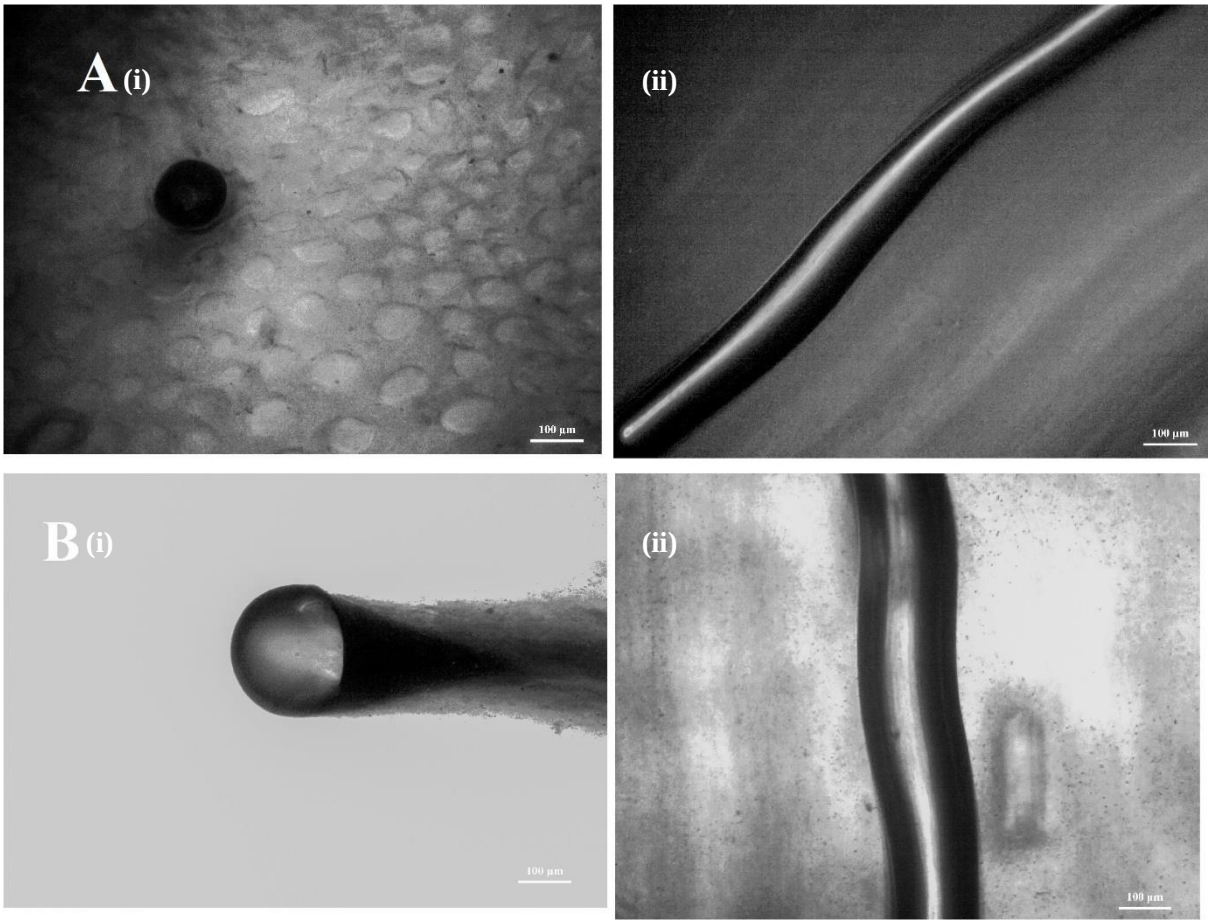

Figure 26: Well defined tubules and pores. **A(i):** Pores formed with 0.6% alginate, diameter =146 µm. **A(ii):** Tubules formed with 0.6% alginate, diameter =150 µm. **B(i)** Pores formed with 0.75% alginate, diameter =220 µm. **B(ii)** Tubules formed with 0.75% alginate, diameter =208 µm

ii. SCANNING ELECTRON MICROSCOPY

Water is the major constituent in the structure of the gel. However, for SEM studies, water has to be removed since the equipment is operated in vacuum. So, the gels had to be dried to remove water from them. The gels were frozen at -20ºC for 2 hours and then

subjected to lyophilisation at -56ºC for 48 hours. The -20ºC freezing damaged the pore structure to a very high extent and thereby, lyophilised samples were not retaining their tubular morphologies. Hence, an alternative drying process was carried out. Very thin sections of scaffold (<1mm) were cut and were subjected to glutaraldehyde fixation for 3 hours. They were then dried in ethanol gradient in vacuum. These samples were then taken for SEM imaging.

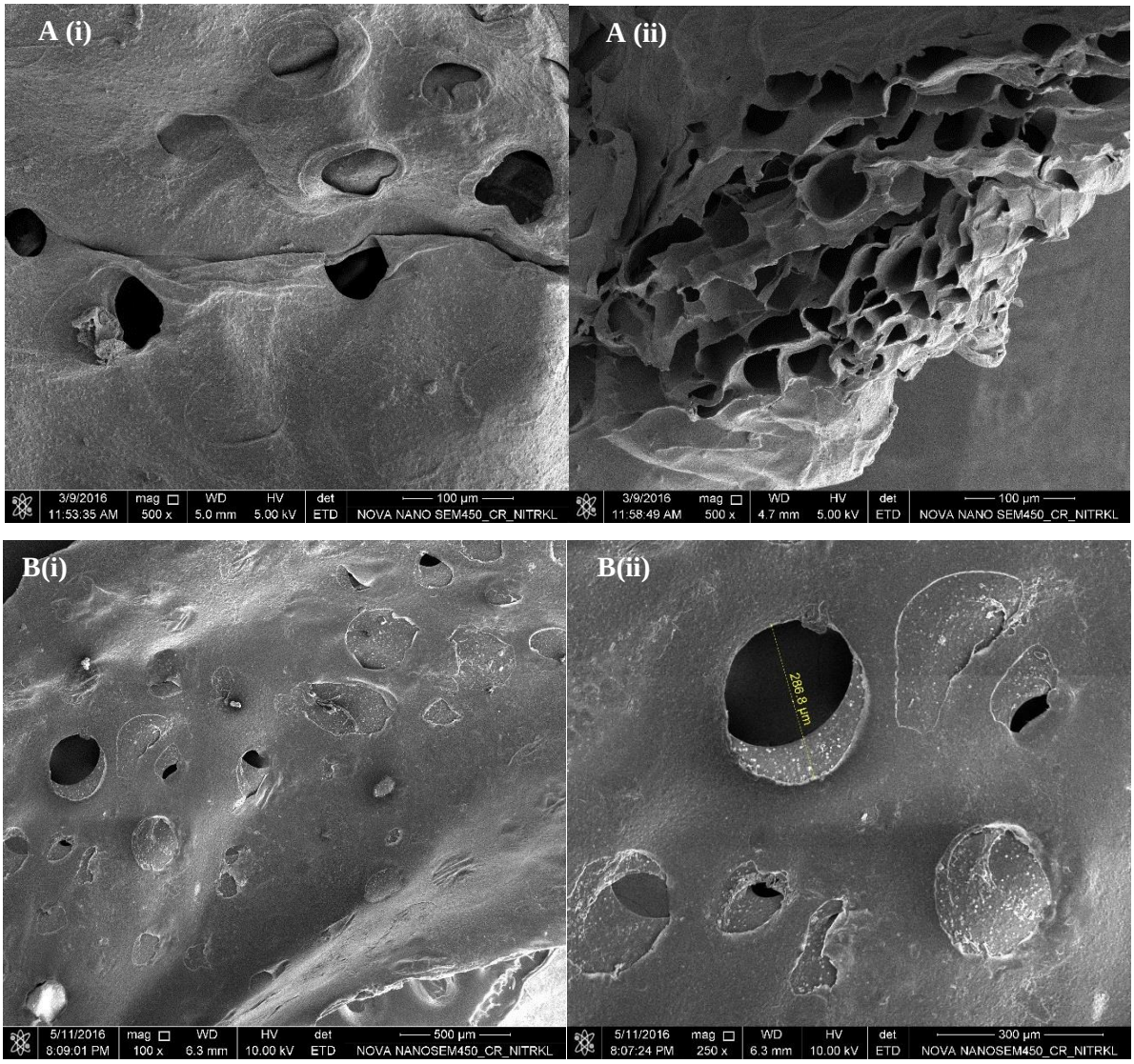

Figure 27: **A:** SEM image of scaffolds where Kimwipes^{TM} were used for primary layer formation and the scaffolds were freeze dried for SEM analysis. **B:** SEM image of pores formed where CaCl2 was sprayed for primary layer formation and the scaffold was fixed in glutaraldehyde and dried in ethanol gradient for SEM analysis.

5.2.2. PHYSIOCHEMICAL CHARACTERISATION

i. SWELLING AND DEGRADATION STUDIES

The most common feature of a gel is that it swells in a thermodynamically stable solvent (Ganji et. al. 2010). Gels prepared with 0.5%, 0.6% and 0.75% alginate solutions and 1M CaCl2 were air dried till no moisture is left on the sample and were subjected to swell in autoclaved PBS.

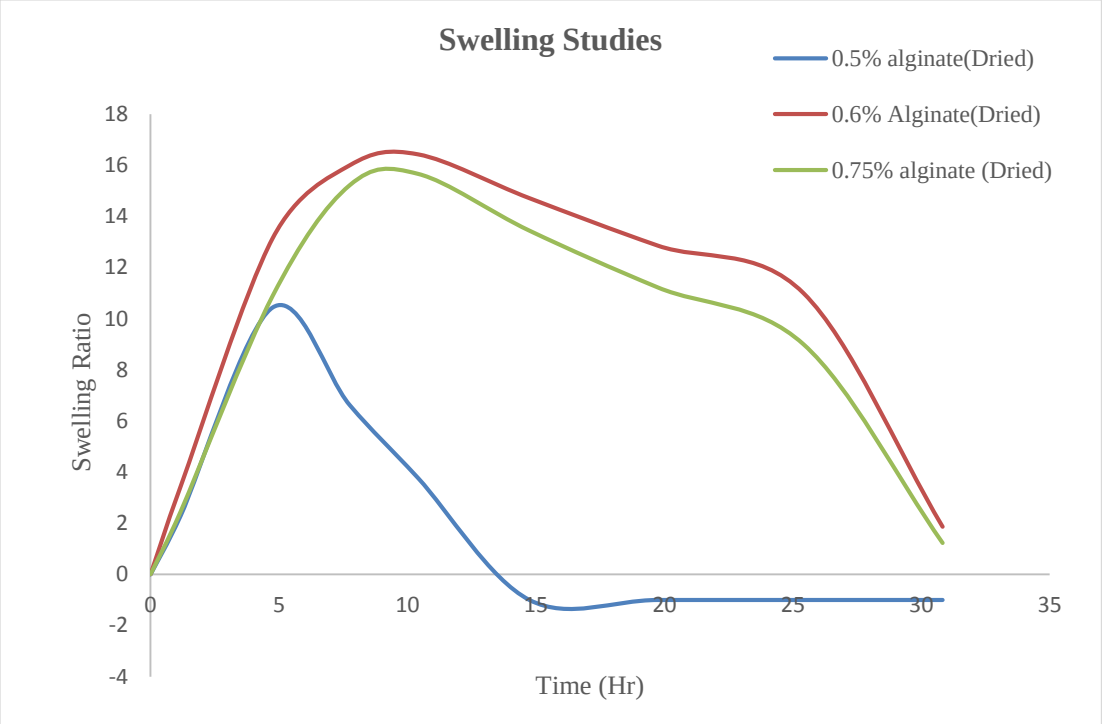

Figure 28: Swelling ratio of gels prepared with 0.5, 0.6 and 0.75% sodium alginate. 0.5% alginate gels degraded faster while 0.6 and 0.75% alginate gels showed similar swelling profiles.

Results showed that 0.5% Alginate gel swelled till the first 5 hours, where it swelled up to 10 times its dry weight and then started to degrade in PBS. Similarly, 0.6% and 0.7% alginate solutions swelled up to 10 hours where they reached 15 times their dry weight. Then, they didn't swell and fairly maintained their weight till 25 hours. After 25 hours, they started degrading in PBS. The degradation of the gels was found to be because of the exchange of Calcium ions in the gel to hydrogen of PBS. Precipitation of Calcium Phosphate was observed which confirms this inference.

ii. FOURIER TRANSFORM INFRARED SPECTROSCOPY

The FTIR spectroscopy had many characteristic alginate peaks. The peak at 3401 cm^{-1} denotes the stretching vibrations of OH bonds. The small peaks at 2907.5 and 2840.5 cm^{-1} represents the Aliphatic CH bonds. The Asymmetric and symmetric stretching of Carboxylate salt is strongly shown at 1616 and 1429 cm^{-1}. The peak at 1083 is the result of Co-Stretching vibration of pyranosyl ring and the peak at 935 cm^{-1} is of the co-stretching with contributions from CCH and COH deformation. The peaks at 1316.5 cm^{-1} was due to C-C stretching and the vibrations of COOH groups.

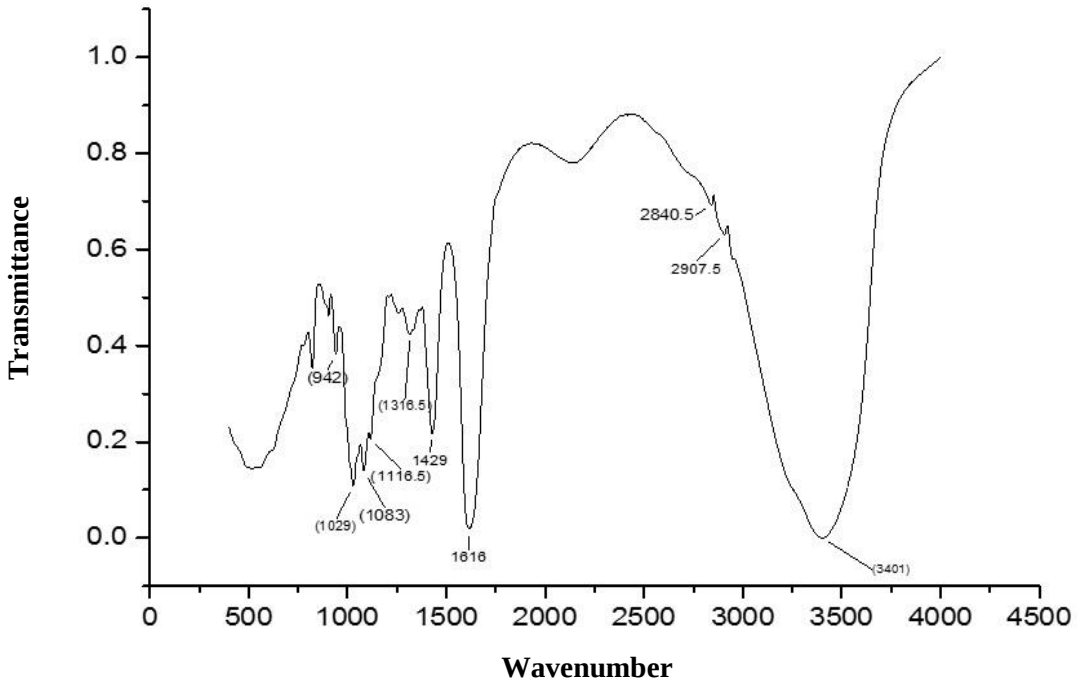

Figure 29: FTIR Spectra of gels prepared with 0.75% sodium alginate and 1M calcium chloride. The transmittance observed was plotted against wave number.

The composition of the polymeric alginate could be determined through FTIR as proposed by Filippov et.al.,1974. The ratio of absorbance at 1320 and 1290 cm^{-1} provided the approximate composition of glucuronic and mannuronic acid in alginate. A_{1320}/A_{1290} was found to be 0.93 by FTIR studies and hence, the respective glucuronic acid and mannuronic acid composition was determined by using the standard curve provided by Filippov et. al.,1974.

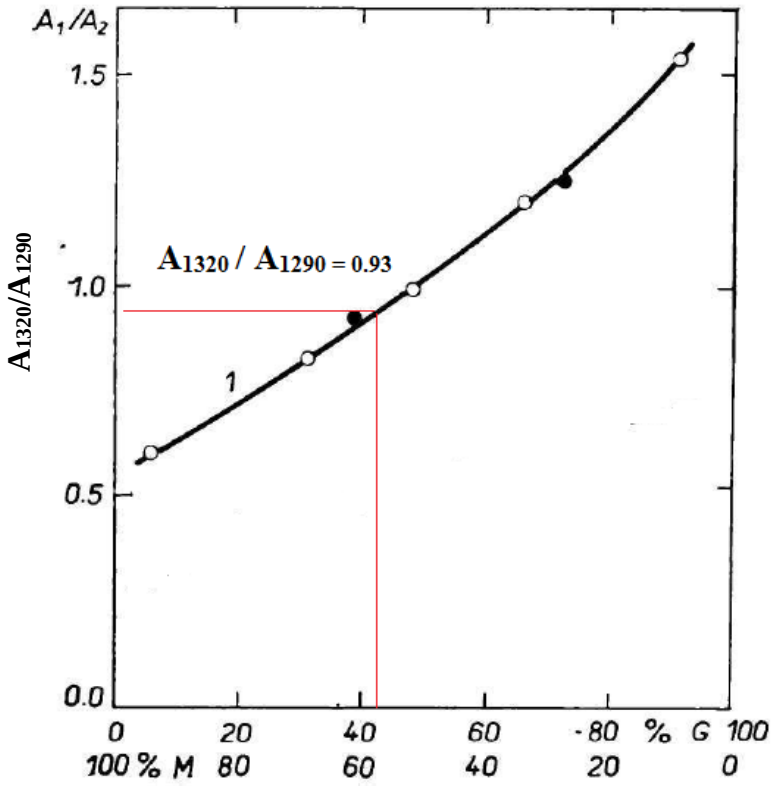

Figure 30: A_{1320}/A_{1290} for alginate. The standard curve was provided by Filippov et. al.,1974. The A_{1320}/A_{1290} of the FTIR spectra was extrapolated against the glucuronic and mannuronic acid concentration in the standard curve.

From the FTIR spectra, it was found that the ratio of A_{1320} and A_{1290} was 0.93. By extrapolating it against the glucuronic and mannuronic acid contents of the standard curve. The glucuronic acid content was found to be 43% and mannuronic acid content was found to be 57% approximately.

iii. MECHANICAL ANALYSIS OF THE SCAFFOLD

Compression testing was done with a trigger load of 0.25 N, test speed of 0.5 mm/s with a TA 44 probe. The force required to compress the sample to a depth of 3 mm was determined using the compression procedure provided in the equipment. Compression testing was done for 0.5%, 0.6% and 0.75% alginate gels made with 1 M $CaCl_2$ solution.

The compressive strength of the gel decreased with the reduction of Alginate concentration. The 0.5% Alginate gel got compressed to 3 mm at 0.8 N, 0.6% Alginate gel compressed 3 mm at 1.74 N and 0.75% Alginate gel compressed to 3 mm at 1.78 N. Thus, 0.75% Alginate gel was found to be stronger with respect to compressive forces.

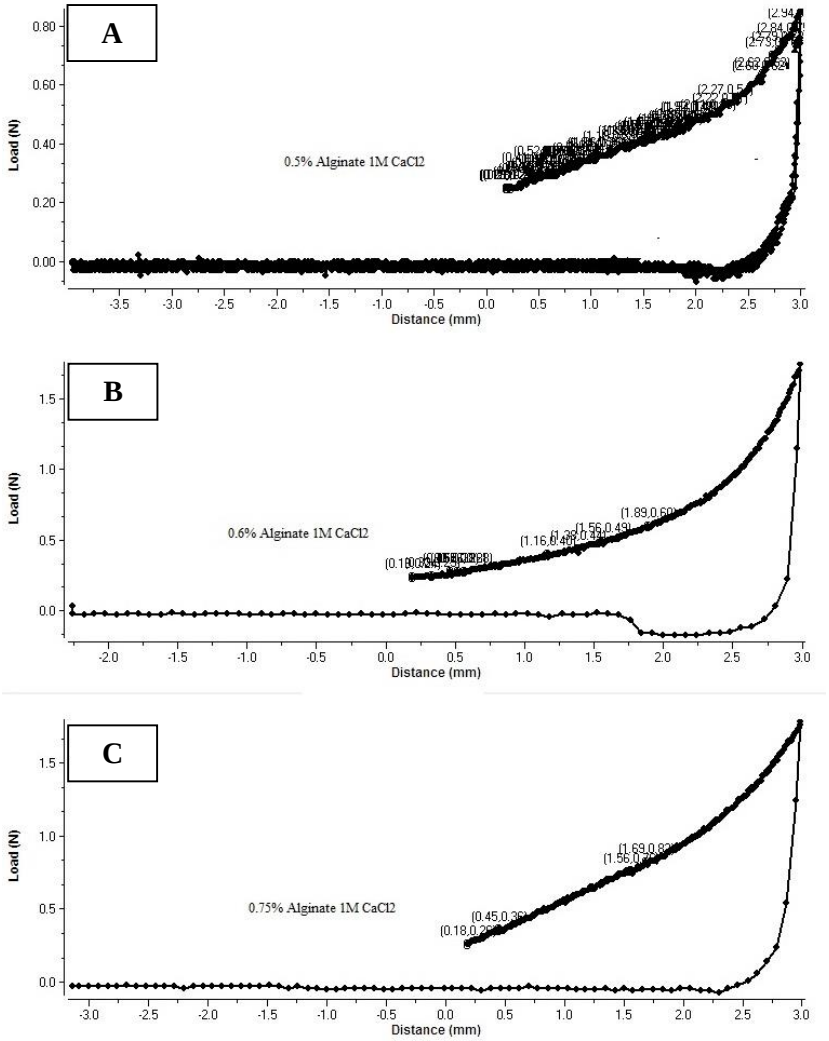

Figure 31: Compressive Strength Analysis of calcium alginate gels. Force required to compress 3mm of 0.5%(A), 0.6%(B) and 0.75%(C) alginate gels were determined.

CHAPTER 6

CONCLUSION

The behavior of Spermatogonia A in the SSC niche of mouse was simulated successfully and the cell counts was validated with a literature that had verified the real counts of Type A spermatogonia in mouse. Using the data of model, a scaffold was designed and developed with anisotropic characteristics and structural morphology related to that of seminiferous tubules. The gels had tubules of diameters from 100 µm to 300 µm which may provide a 3D environment for the growth and differentiation of SSCs. The behavior of SSCs in the 3D environment provided by calcium alginate gels can be monitored by using the Simulation. A software was also developed to predict the dose and concentration of SSCs required for seeding the scaffold. Future studies should optimize the scaffolds to be used in human testicular tissue engineering for in vitro spermatogenesis and/or development of prosthesis.

REFERENCE

1. Oakberg, E. F. "Spermatogonial stem-cell renewal in the mouse." *The Anatomical Record* 169, no. 3 (1971): 515-531.

2. DE ROOIJ, DIRK G. "Stem cells in the testis." *International journal of experimental pathology* 79, no. 2 (1998): 67-80.

3. De Rooij, D. G. "Proliferation and differentiation of undifferentiated spermatogonia in the mammalian testis." *Stem Cells. Their Identification and Characterisation (CS Potten, Ed.), Churchill Livingstone, Edinburgh* (1983): 89-117.

4. Russell, Lonnie Dee. *Histological and histopathological evaluation of the testis*. Cache River Press, 1990.

5. de Rooij, Dirk G., and Maria EAB van Beek. "Computer simulation of the rodent spermatogonial stem cell niche." *Biology of reproduction* 88, no. 5 (2013): 131.

6. Chiarini-Garcia, H., A. M. Raymer, and L. D. Russell. "Non-random distribution of spermatogonia in rats: evidence of niches in the seminiferous tubules." *Reproduction* 126, no. 5 (2003): 669-680.

7. Yoshida, Shosei, Mamiko Sukeno, and Yo-ichi Nabeshima. "A vasculature-associated niche for undifferentiated spermatogonia in the mouse testis." *Science* 317, no. 5845 (2007): 1722-1726.

8. Ellis, Sarah L., Jochen Grassinger, Allan Jones, Judy Borg, Todd Camenisch, David Haylock, Ivan Bertoncello, and Susan K. Nilsson. "The relationship between bone, hemopoietic stem cells, and vasculature." *Blood* 118, no. 6 (2011): 1516-1524.

9. Russell, L. D., and R. N. Peterson. "Determination of the elongate spermatid—Sertoli cell ratio in various mammals." *Journal of reproduction and fertility* 70, no. 2 (1984): 635-641.

10. RUSSELL, LONNIE D., LINDA E. ALGER, and LYNN G. NEQUIN. "Hormonal control of pubertal spermatogenesis." *Endocrinology* 120, no. 4 (1987): 1615-1632.

11. Lok, D., D. Weenk, and D. G. De Rooij. "Morphology, proliferation, and differentiation of undifferentiated spermatogonia in the Chinese hamster and the ram." *The Anatomical Record* 203, no. 1 (1982): 83-99.

12. De Rooij, D. G., and J. M. Janssen. "Regulation of the density of spermatogonia in the seminiferous epithelium of the Chinese hamster: I. Undifferentiated spermatogonia." *The Anatomical Record* 217, no. 2 (1987): 124-130.

13. Su, Jing, Pedro J. Zapata, Chien-Chiang Chen, and J. Carson Meredith. "Local cell metrics: a novel method for analysis of cell-cell interactions." *BMC bioinformatics* 10, no. 1 (2009): 350.

14. de Rooij, Dirk G. "Proliferation and differentiation of spermatogonial stem cells." *Reproduction* 121, no. 3 (2001): 347-354.

15. Rooij, D. G., D. Lok, and D. Weenk. "Feedback regulation of the proliferation of the undifferentiated spermatogonia in the Chinese hamster by the differentiating spermatogonia." *Cell Proliferation* 18, no. 1 (1985): 71-81.

16. Nakagawa, Toshinori, Yo-ichi Nabeshima, and Shosei Yoshida. "Functional identification of the actual and potential stem cell compartments in mouse spermatogenesis." *Developmental cell* 12, no. 2 (2007): 195-206.

17. Nakagawa, Toshinori, Manju Sharma, Yo-ichi Nabeshima, Robert E. Braun, and Shosei Yoshida. "Functional hierarchy and reversibility within the murine spermatogenic stem cell compartment." *Science* 328, no. 5974 (2010): 62-67.

18. Lok, D., and D. G. De Rooij. "Spermatogonial multiplication in the Chinese hamster. III. Labelling indices of undifferentiated spermatogonia throughout the cycle of the seminiferous epithelium." *Cell and tissue kinetics* 16, no. 1 (1983): 31-40.

19. Oakberg, Eugene F. "A description of spermiogenesis in the mouse and its use in analysis of the cycle of the seminiferous epithelium and germ cell renewal." *American Journal of Anatomy* 99, no. 3 (1956): 391-413.

20. Huckins, Claire. "Cell cycle properties of differentiating spermatogonia in adult Sprague-Dawley rats." *Cell Proliferation* 4, no. 2 (1971): 139-154.

21. Clermont, Yves, and Louis Hermo. "Spermatogonial stem cells in the albino rat." *American Journal of Anatomy* 142, no. 2 (1975): 159-175.

22. ROOIJ, DIRK G., and LONNIE D. RUSSELL. "All you wanted to know about spermatogonia but were afraid to ask." *Journal of andrology* 21, no. 6 (2000): 776-798.

23. De Rooij, D. G., and F. M. F. van Dissel-Emiliani. "Regulation of proliferation and differentiation of stem cells in the male germ line." *Stem Cells* (1997): 283-313.

24. Bendel–Stenzel, Michael, Robert Anderson, Janet Heasman, and Chris Wylie. "The origin and migration of primordial germ cells in the mouse." In *Seminars in cell & developmental biology*, vol. 9, no. 4, pp. 393-400. Academic Press, 1998.

25. Khil, Pavel P., Natalya A. Smirnova, Peter J. Romanienko, and R. Daniel Camerini-Otero. "The mouse X chromosome is enriched for sex-biased genes not subject to selection by meiotic sex chromosome inactivation." *Nature genetics* 36, no. 6 (2004): 642-646.

26. Russell, Lonnie D. "Sertoli-germ cell interrelations: A review." *Gamete Research* 3, no. 2 (1980): 179-202.

27. McLachlan, R., N. Wreford, et al. (1996). "The endocrine regulation of spermatogenesis: independent roles for testosterone and FSH." Journal of Endocrinology **148**(1): 1-9.
28. Hess, R. A. and L. R. de Franca (2008). Spermatogenesis and cycle of the seminiferous epithelium. Molecular mechanisms in spermatogenesis, Springer**:** 1-15.

29. Lee, J. H., H. J. Kim, et al. (2006). "In vitro spermatogenesis by three-dimensional culture of rat testicular cells in collagen gel matrix." Biomaterials **27**(14): 2845-2853.

30. Reuter, K., S. Schlatt, et al. (2012). "Fact or fiction: in vitro spermatogenesis." Spermatogenesis **2**(4): 245-252.

31. Sato, T., T. Yokonishi, et al. (2012). "Testis tissue explantation cures spermatogenic failure in c-Kit ligand mutant mice." Proceedings of the National Academy of Sciences **109**(42): 16934-16938

32. Mehraein, Fereshteh, and Feraidoon Negahdar. "Morphometric evaluation of seminiferous tubules in aged mice testes after melatonin administration." *Cell Journal (Yakhteh)* 13, no. 1 (2011): 1.

33. Morales, E., R. Horn, L. M. Pastor, L. Santamaria, J. Pallarés, A. Zuasti, C. Ferrer, and M. Canteras. "Involution of seminiferous tubules in aged hamsters: an ultrastructural, immunohistochemical and quantitative morphological study." (2004).

34. Eslahi, Neda, Mahmoud Reza Hadjighassem, Mohammad Taghi Joghataei, Tooba Mirzapour, Mehrdad Bakhtiyari, Malak Shakeri, Vahid Pirhajati, Peymaneh Shirinbayan, and Morteza Koruji. "The effects of poly L-lactic acid nanofiber scaffold on mouse spermatogonial stem cell culture." *International journal of nanomedicine* 8 (2013): 4563.

35. Oakberg, Eugene F. "Duration of spermatogenesis in the mouse and timing of stages of the cycle of the seminiferous epithelium." *American Journal of Anatomy* 99, no. 3 (1956): 507-516.

36. Nagano, Makoto, Mary R. Avarbock, and Ralph L. Brinster. "Pattern and kinetics of mouse donor spermatogonial stem cell colonization in recipient testes." *Biology of reproduction* 60, no. 6 (1999): 1429-1436.

37. Brinster, Ralph L., and James W. Zimmermann. "Spermatogenesis following male germ-cell transplantation." *Proceedings of the National Academy of Sciences* 91, no. 24 (1994): 11298-11302.

38. Boer, P., M. Vries, and L. Ramos. "A mutation study of sperm head shape and motility in the mouse: lessons for the clinic." *Andrology* 3, no. 2 (2015): 174-202.

39. Yamamoto, Masaya, Daylon James, Hui Li, Jason Butler, Shahin Rafii, and Sina Rabbany. "Generation of stable co-cultures of vascular cells in a honeycomb alginate scaffold." *Tissue Engineering Part A* 16, no. 1 (2009): 299-308.

40. Grant, Gregor T., Edwin R. Morris, David A. Rees, Peter JC Smith, and David Thom. "Biological interactions between polysaccharides and divalent cations: the egg-box model." *FEBS letters* 32, no. 1 (1973): 195-198.

41. McHugh, Dennis J. "Production, properties and uses of alginates." *Production and Utilization of Products from Commercial Seaweeds. FAO. Fish. Tech. Pap* 288 (1987): 58-115.

42. Documentation, Matlab. "The MathWorks Inc." (2005).

43. Matson, Clinton K., Mark W. Murphy, Michael D. Griswold, Shosei Yoshida, Vivian J. Bardwell, and David Zarkower. "The mammalian doublesex homolog DMRT1 is a transcriptional gatekeeper that controls the mitosis versus meiosis decision in male germ cells." *Developmental cell* 19, no. 4 (2010): 612-624.

44. Hermann, Brian P., Meena Sukhwani, Marc C. Hansel, and Kyle E. Orwig. "Spermatogonial stem cells in higher primates: are there differences from those in rodents?." *Reproduction* 139, no. 3 (2010): 479-493.

45. Filippov, M. P., and R. Kohn. "Determination of composition of alginates by infrared spectroscopic method." *Chem zvesti* 28, no. 6 (1974): 817-819.

46. Sun, Zhenxing, Mingxing Xie, Feixiang Xiang, Yue Song, Cheng Yu, Yanrong Zhang, Sachin Ramdhany, and Jing Wang. "Utility of Real-Time Shear Wave Elastography in the Assessment of Testicular Torsion." *PloS one* 10, no. 9 (2015): e0138523.

47. Duck, Francis A. Physical properties of tissues: a comprehensive reference book. Academic press, 2013.

48. Mcintosh, Robert L., and Vitas Anderson. "A comprehensive tissue properties database provided for the thermal assessment of a human at rest." *Biophysical Reviews and Letters* 5, no. 03 (2010): 129-151.

49. Nogueira, D., C. Bourgain, G. Verheyen, and A. C. Van Steirteghem. "Light and electron microscopic analysis of human testicular spermatozoa and spermatids from frozen and thawed testicular biopsies." *Human Reproduction* 14, no. 8 (1999): 2041-2049.

50. Le Novère, Nicolas. "Quantitative and logic modelling of molecular and gene networks." *Nature Reviews Genetics* 16, no. 3 (2015): 146-158.

51. Whillis, James. *Gray's anatomy: descriptive and applied*. Edited by Thomas Baillie Johnston. London: Longmans, 1954.

52. Shetty, Gunapala, and Marvin L. Meistrich. "The missing niche for spermatogonial stem cells: do blood vessels point the way?." *Cell Stem Cell* 1, no. 4 (2007): 361-363.

53. Moussouni, Fouzia, Laure Berti-Équille, and France le Développement. "Cleaning, Integrating, and Warehousing Genomic Data From Biomedical Resources." *Biological Knowledge Discovery Handbook: Preprocessing, Mining, and Postprocessing of Biological Data* (2013): 35-58.

54. Imboden, Dieter M., and Stefan Pfenninger. *Introduction to systems analysis: mathematically modeling natural systems*. Springer Science & Business Media, 2012.

55. Sujansky, Walter. "Heterogeneous database integration in biomedicine." *Journal of biomedical informatics* 34, no. 4 (2001): 285-298.

56. Pavé, Alain. "Necessity of chance: biological roulettes and biodiversity." *Comptes rendus biologies* 330, no. 3 (2007): 189-198.

57. Morange, M., 2001. Past Times A successful form of reductionism: a historical perspective. *BIOCHEMIST*, *23*(6), pp.37-39.

58. Van Regenmortel, Marc HV. "Reductionism and complexity in molecular biology." *EMBO reports* 5, no. 11 (2004): 1016-1020.

59. Jankowski, M.D., Williams, C.J., Fair, J.M. and Owen, J.C., 2013. Birds shed RNA-viruses according to the Pareto Principle. *PloS one*, *8*(8), p.e72611.
60. Wynn, Michelle L., Nikita Consul, Sofia D. Merajver, and Santiago Schnell. "Logic-based models in systems biology: a predictive and parameter-free network analysis method." *Integrative biology* 4, no. 11 (2012): 1323-1337.

61. Aittokallio, Tero, and Benno Schwikowski. "Graph-based methods for analysing networks in cell biology." *Briefings in bioinformatics* 7, no. 3 (2006): 243-255.

62. Hinegardner, Ralph, and Joseph Engelberg. "Biological complexity." *Journal of Theoretical Biology* 104, no. 1 (1983): 7-20.

63. Wooley, J. C., and H. S. Lin. "Catalyzing Inquiry at the Interface of Computing and Biology. Committee on Frontiers at the Interface of Computing and Biology, National Research Council." *Committee on Frontiers at the Interface of Computing and Biology, National Research Council* (2005).

64. Sloutsky, Roman, Nicolas Jimenez, S. Joshua Swamidass, and Kristen M. Naegle. "Accounting for noise when clustering biological data." *Briefings in bioinformatics* 14, no. 4 (2013): 423-436.

65. Birkland, Aaron, and Golan Yona. "BIOZON: a hub of heterogeneous biological data." *Nucleic acids research* 34, no. suppl 1 (2006): D235-D242.

66. Ganji, F., Vasheghani-Farahani, S. and Vasheghani-Farahani, E., 2010. Theoretical description of hydrogel swelling: a review. *Iran Polym J*, *19*(5), pp.375-398.

ANNEXURE I

SOURCE CODE

runme.m

```
clear;clc;
run seminiferoustubule1
run seeding2
run findingrowcolumn3
srdensfac=10;
dfdensfac=1000;
n=input('number of cycles:');
densfordiv=input(' maximum density for division? :(Default = 0.14)');
maxdensmig=input(' Enter the maximum density above which cell wont migrate :(Default = 0.37) ');
mindensmig=input(' Enter the minimum density below which cell wont migrate: (Default = 0.007) ');
mindensdivmig=input(' Enter the minimum density below which cell wont migrate during division: (Default = 0.0) ');
maxdensdivmig=input(' Enter the maximum density above which cell wont migrate during division: (Default = 0.025) ');
migdensfac=10;
run cellmigration
difftag=zeros(80,170);
stag=zeros(80,170);
while round(sum(sum(As))/10)<4
   run celldivision
end
imwrite(As/16,'repopulated.png');
pt=As;
Harvest=zeros(n,16);
cellAs=zeros(n,10);
cellApr=zeros(n,10);
cellAal4=zeros(n,10);
cellAal8=zeros(n,10);
cellAal16=zeros(n,10);
for epcycle=1:n
   for divcycle=1:3
      divcycle
      if divcycle<3
         run decisiondivdif
         run steadystate
         run celldivision
      end
      if divcycle==3
         run decisiondivdif
         run steadystate
         hardensfac=100;
[As,u]=divisionr(As,difftag,0.6,u,densfordiv,mindensdivmig,maxdensdivmig,denscc);%,hardensfac);
         imwrite(As/16,num2str(u),'png');
         u=u+1;
         run harvest
         run cellnumber
      end
   end
   epcycle
end
run totalcell
run excelexport
endtime=clock;
save data.mat
```

ACCESSORY FILES

seminiferoustubule1.m

```
% creating the niche area
starttime=clock;
denscc=1;
semtubule=zeros(80,170);
migrationtag=zeros(80,170);
lintag=zeros(80,170);
Psr=semtubule;
u=1;
for m=1:35
   Psr(m,51)=60;
   Psr(m,52)=80;
   Psr(m,53)=80;
   Psr(m,58)=80;
   Psr(m,59)=80;
   Psr(m,60)=60;
end
for m=36:37;
   Psr(m,52)=80;
```

```
    Psr(m,53)=80;
    Psr(m,58)=80;
    Psr(m,59)=80;
end
for m=1:35
    Psr(m,111)=60;
    Psr(m,112)=80;
    Psr(m,113)=80;
    Psr(m,118)=80;
    Psr(m,119)=80;
    Psr(m,120)=60;
end
for m=36:37
    Psr(m,112)=80;
    Psr(m,113)=80;
    Psr(m,118)=80;
    Psr(m,119)=80;
end
for m=46:80
    Psr(m,51)=60;
    Psr(m,52)=80;
    Psr(m,53)=80;
    Psr(m,58)=80;
    Psr(m,59)=80;
    Psr(m,60)=60;
end
for m=44:45
    Psr(m,52)=80;
    Psr(m,53)=80;
    Psr(m,58)=80;
    Psr(m,59)=80;
end
for m=46:80
    Psr(m,111)=60;
    Psr(m,112)=80;
    Psr(m,113)=80;
    Psr(m,118)=80;
    Psr(m,119)=80;
    Psr(m,120)=60;
end
for m=44:45
    Psr(m,112)=80;
    Psr(m,113)=80;
    Psr(m,118)=80;
    Psr(m,119)=80;
end
for m=36
    for n=1:51
        Psr(m,n)=60;
    end
    for n=60:111
        Psr(m,n)=60;
    end
    for n=120:170
        Psr(m,n)=60;
    end
end
for m=45
    for n=1:51
        Psr(m,n)=60;
    end
    for n=60:111
        Psr(m,n)=60;
    end
    for n=120:170
        Psr(m,n)=60;
    end
end
for m=37:38
    for n=1:53
        Psr(m,n)=80;
    end
    for n=58:113
        Psr(m,n)=80;
    end
    for n=118:170
        Psr(m,n)=80;
    end
end
for m=43:44
    for n=1:53
        Psr(m,n)=80;
    end
    for n=58:113
        Psr(m,n)=80;
    end
```

```
    for n=118:170
        Psr(m,n)=80;
    end
end
for m=39:42
    for n=1:170
        Psr(m,n)=90;
    end
end
for m=1:80
    for n=54:57
        Psr(m,n)=90;
    end
    for n=114:117
        Psr(m,n)=90;
    end
end
for m=1:80
    for n=1:170
        if Psr(m,n)==0
            Psr(m,n)=10;
        end
    end
end
display('niche is created');
imwrite(Psr/100,num2str(u),'png');
imwrite(Psr/100,'nicheassumed.png');
u=u+1;
Qsr=zeros(80,170);
```

seeding2.m

```
[a,b]=size(Psr);
seednic=zeros(80,170);
As=zeros(80,170);
for i=1:a
    for j=1:b
        if Psr(i,j)==90
            seednic(i,j)=rand(1);
            if seednic(i,j)<0.01 && seednic(i,j)>0
                As(i,j)=1;
            end
        end
    end
end
Aseeding=As;
display('seeding is done');
imwrite(Aseeding/16,num2str(u),'png');
u=u+1;
```

findingrowcolumn3.m

```
[rowAs,columnAs]=celllocation(As);
display('row and column are located');
```

cellmigration.m

```
[rowAs,columnAs]=celllocation(As);
distbtw=zeros(length(rowAs),length(rowAs));
mdist=0;
dencm=ones(80,170);
while mdist<3
    [rowAs,columnAs]=celllocation(As);
    Densdivm=zeros(1,length(rowAs));
    for i=1:length(rowAs)
        if As(rowAs(i),columnAs(i))==1

Densdivm(i)=densityrc(As,rowAs(i),columnAs(i),dencm);
        end
    end
    [g,M]=max(Densdivm);
    Astm=As;

[As]=migration(As,rowAs(M),columnAs(M),mindensmig,maxd
ensmig,denscc);
    if Astm==As
        break;
    end
    for i=1:length(rowAs)
        for j=1:length(rowAs)
distbtw(i,j)=distancefun(rowAs(i),columnAs(i),rowAs(j),column
As(j));
            if distbtw(i,j)==0
                distbtw(i,j)=1000;
            end
        end
    end
    mdist=min(min(distbtw));
    imwrite(As/16,num2str(u),'png');
    u=u+1;
end
```

celldivision.m

```
clear randcd;
```

```
clear ran;
clear maxim;
clear rowAs;
clear columnAs;
[drowAs,dcolumnAs]=celllocation(As);
randcd=rand(1,length(drowAs));
ran=zeros(1,length(drowAs));
ptag=zeros(80,170);
for i=1:length(drowAs)
   [maxim,ran(i)]=max(randcd);
   randcd(ran(i))=0;
end
for i = 1:length(drowAs)
   if difftag(drowAs(i),dcolumnAs(i))==1 &&
As(drowAs(i),dcolumnAs(i))==1
As(drowAs(i),dcolumnAs(i))=As(drowAs(i),dcolumnAs(i))*2;
      if As(drowAs(i),dcolumnAs(i))>2
         display('bruh');
      end
   end
    if As(drowAs(i),dcolumnAs(i))>1
As(drowAs(i),dcolumnAs(i))=As(drowAs(i),dcolumnAs(i))*2;
   end
end
for id=1:length(ran)
   if difftag(drowAs(ran(id)),dcolumnAs(ran(id)))==0 &&
As(drowAs(ran(id)),dcolumnAs(ran(id)))==1
  if stag(drowAs(ran(id)),dcolumnAs(ran(id))) ~= 1
[As,u]=division(As,drowAs(ran(id)),dcolumnAs(ran(id)),u,densf
ordiv,mindensdivmig,maxdensdivmig,denscc,6); %srdensfac);
         imwrite(As/16,num2str(u),'png');
         u=u+1;
         [rowAs,columnAs]=celllocation(As);
         clear migdensfac;
         migdensfac=1;
         run cellmigration
      end
      if stag(drowAs(ran(id)),dcolumnAs(ran(id))) == 1
         denu=zeros(80,170);
[As,u]=division(As,drowAs(ran(id)),dcolumnAs(ran(id)),u,densf
ordiv,mindensdivmig,maxdensdivmig,denscc,8); %,dfdensfac);
         imwrite(As/16,num2str(u),'png');
         u=u+1;
         [rowAs,columnAs]=celllocation(As);
         clear migdensfac;
         migdensfac=1;
         run cellmigration
      end
   end
end
```

cellnumber.m

```
[rownum,columnnum]=celllocation(As);
for inu=1:length(columnnum)
   if As(rownum(inu),columnnum(inu))==1
      if Psr(rownum(inu),columnnum(inu))==90
         cellAs(epcycle,9)=cellAs(epcycle,9)+1;
      end
       if Psr(rownum(inu),columnnum(inu))==80
         cellAs(epcycle,8)=cellAs(epcycle,8)+1;
       end
       if Psr(rownum(inu),columnnum(inu))==60
         cellAs(epcycle,6)=cellAs(epcycle,6)+1;
       end
       if Psr(rownum(inu),columnnum(inu))==10
         cellAs(epcycle,1)=cellAs(epcycle,1)+1;
       end
   end
   if As(rownum(inu),columnnum(inu))==2
      if Psr(rownum(inu),columnnum(inu))==90
         cellApr(epcycle,9)=cellApr(epcycle,9)+1;
      end
      if Psr(rownum(inu),columnnum(inu))==80
         cellApr(epcycle,8)=cellApr(epcycle,8)+1;
      end
      if Psr(rownum(inu),columnnum(inu))==60
         cellApr(epcycle,6)=cellApr(epcycle,6)+1;
      end
      if Psr(rownum(inu),columnnum(inu))==10
         cellApr(epcycle,1)=cellApr(epcycle,1)+1;
      end
   end
   if As(rownum(inu),columnnum(inu))==4
      if Psr(rownum(inu),columnnum(inu))==90
         cellAal4(epcycle,9)=cellAal4(epcycle,9)+1;
      end
      if Psr(rownum(inu),columnnum(inu))==80
         cellAal4(epcycle,8)=cellAal4(epcycle,8)+1;
      end
      if Psr(rownum(inu),columnnum(inu))==60
```

```
        cellAal4(epcycle,6)=cellAal4(epcycle,6)+1;
      end
      if Psr(rownum(inu),columnnum(inu))==10
        cellAal4(epcycle,1)=cellAal4(epcycle,1)+1;
      end
    end
    if As(rownum(inu),columnnum(inu))==8
      if Psr(rownum(inu),columnnum(inu))==90
        cellAal8(epcycle,9)=cellAal8(epcycle,9)+1;
      end
      if Psr(rownum(inu),columnnum(inu))==80
        cellAal8(epcycle,8)=cellAal8(epcycle,8)+1;
      end
      if Psr(rownum(inu),columnnum(inu))==60
        cellAal8(epcycle,6)=cellAal8(epcycle,6)+1;
      end
      if Psr(rownum(inu),columnnum(inu))==10
        cellAal8(epcycle,1)=cellAal8(epcycle,1)+1;
      end
    end
    if As(rownum(inu),columnnum(inu))==16
      if Psr(rownum(inu),columnnum(inu))==90
        cellAal16(epcycle,9)=cellAal16(epcycle,9)+1;
      end
      if Psr(rownum(inu),columnnum(inu))==80
        cellAal16(epcycle,8)=cellAal16(epcycle,8)+1;
      end
      if Psr(rownum(inu),columnnum(inu))==60
        cellAal16(epcycle,6)=cellAal16(epcycle,6)+1;
      end
      if Psr(rownum(inu),columnnum(inu))==10
        cellAal16(epcycle,1)=cellAal16(epcycle,1)+1;
      end
    end
  end
```

decisiondivdiff.m

```
clear As60;
clear As90;
clear As80;
clear As10;
clear difftag;
[irowAs,icolumnAs]=celllocation(As);
[irAs,icAs]=cellocAs(As);
As90=zeros(80,170);
As80=zeros(80,170);
As60=zeros(80,170);
As10=zeros(80,170);
difftag=zeros(80,170);
for i=1:length(irowAs)
   if Psr(irowAs(i),icolumnAs(i))==90
As90(irowAs(i),icolumnAs(i))=As(irowAs(i),icolumnAs(i));
   end
   if Psr(irowAs(i),icolumnAs(i))==80

As80(irowAs(i),icolumnAs(i))=As(irowAs(i),icolumnAs(i));
   end
   if Psr(irowAs(i),icolumnAs(i))==60
As60(irowAs(i),icolumnAs(i))=As(irowAs(i),icolumnAs(i));
   end
   if Psr(irowAs(i),icolumnAs(i))==10
As10(irowAs(i),icolumnAs(i))=As(irowAs(i),icolumnAs(i));
   end
end
if sum(sum(As90==1)) > 0
   [rowAs90,columnAs90]=cellocAs(As90);
   rand90=rand(1,length(rowAs90));
   nos90=round(0.1*(length(rowAs90)));
   if nos90 > 0
      for i=1:nos90
         [c,ind90]=max(rand90);
         difftag(rowAs90(ind90),columnAs90(ind90))=1;
         rand90(ind90)=0;
      end
   end
end
if sum(sum(As80==1)) > 0
   [rowAs80,columnAs80]=cellocAs(As80);
   rand80=rand(1,length(rowAs80));
   nos80=round(0.2*length(rowAs80));
   if nos80 > 0
      for i=1:nos80
         [c,ind80]=max(rand80);
         difftag(rowAs80(ind80),columnAs80(ind80))=1;
         rand80(ind80)=0;
      end
   end
end
```

```
if sum(sum(As60==1))>0
   [rowAs60,columnAs60]=cellocAs(As60);
   rand60=rand(1,length(rowAs60));
   nos60=round(0.4*length(rowAs60));
   if nos60 > 0
      for i=1:nos60
         [c,ind60]=max(rand60);
         difftag(rowAs60(ind60),columnAs60(ind60))=1;
         rand60(ind60)=0;
      end
   end
end
if sum(sum(As10==1))>0
   [rowAs10,columnAs10]=cellocAs(As10);
   rand10=rand(1,length(rowAs10));
   nos10=round(0.9*length(rowAs10));
   if nos10 > 0
      for i=1:nos10
         [c,ind10]=max(rand10);
         difftag(rowAs10(ind10),columnAs10(ind10))=1;
         rand10(ind10)=0;
      end
   end
end
```

excelexport.m

```
xlswrite('cellcount.xls',cellAs,'cellAsCount');
xlswrite('cellcount.xls',cellApr,'cellAprCount');
xlswrite('cellcount.xls',cellAal4,'cellAal4Count');
xlswrite('cellcount.xls',cellAal8,'cellAal8Count');
xlswrite('cellcount.xls',cellAal16,'cellAal16Count');
xlswrite('cellcount.xls',Harvest,'cellHarvestCount');
xlswrite('cellcount.xls',Totalcellcount,'TotalCells');
```

harvest.m

```
nos4=0;
for i=1:80
   for j=1:170
      if As(i,j)==8
         As(i,j)=0;
         Harvest(epcycle,8)=Harvest(epcycle,8)+1;
      end
      if As(i,j)==16
         As(i,j)=0;
         Harvest(epcycle,16)=Harvest(epcycle,16)+1;
      end
      if As(i,j)==4
         nos4=nos4+1;
      end
   end
end
if nos4~=0
   [rowAal4,columnAal4]=cellocAal4(As);
   randhar=rand(1,length(rowAal4));
   ranh=zeros(1,length(rowAal4));
   for i=1:length(rowAal4)
      [maxim,ranh(i)]=max(randhar);
      randhar(ranh(i))=0;
   end
   for i=1:round(length(randhar)/2)
      As(rowAal4(ranh(i)),columnAal4(ranh(i)))=0;
      Harvest(epcycle,4)=Harvest(epcycle,4)+1;
   end
end
imwrite(As/16,num2str(u),'png');
u=u+1;
display('harvest done');
```

steadystate.m

```
[rowAs,columnAs]=celllocation(As);
stag=zeros(80,170);
denstt=ones(80,170);
for i=1:length(rowAs)
   densr(i)=densityrc(As,rowAs(i),columnAs(i),denstt);%,1);
end
for i=1:length(densr)
   if densr(i)== 0
      densr(i)=0.000000000001;
   end
end
for i=1:length(densr)
   [c,I]=max(densr);
   denssort(i)=I;
   densr(I)=0;
end
noss=floor(length(rowAs)/2);
for i=1:noss
   stag(rowAs(denssort(i)),columnAs(denssort(i)))=1;
```

```
end
```

totalcell.m

```
for i=1:n
Totalstemcell(i,1)=sum(cellAs(i,1:10))+sum(cellApr(i,:))+sum(cellAal4(i,:))+sum(cellAal8(i,:))+sum(cellAal16(i,:));
   Totalcellcount(i,1)=Totalstemcell(i,1)+sum(Harvest(i,:));
end
```

FUNCTIONS

celllocation.m

```
function [x,y]=celllocation(z)
[a,b]=size(z);
k=0;
for i=1:a
   for j=1:b
      if z(i,j)~=0
         k=k+1;
         x(k)=i;
         y(k)=j;
      end
   end
end
end
```

cellocAal4.m

```
function [x,y]=cellocAal4(z)
[a,b]=size(z);
k=0;
for i=1:a
   for j=1:b
      if z(i,j)==4
         k=k+1;
         x(k)=i;
         y(k)=j;
      end
   end
end
end
```

cellocAal8.m

```
function [x,y]=cellocAal8(z)
[a,b]=size(z);
k=0;
for i=1:a
   for j=1:b
      if z(i,j)==8
         k=k+1;
         x(k)=i;
         y(k)=j;
      end
   end
end
end
```

cellocAal16.m

```
function [x,y]=cellocAal16(z)
[a,b]=size(z);
k=0;
for i=1:a
   for j=1:b
      if z(i,j)==16
         k=k+1;
         x(k)=i;
         y(k)=j;
      end
   end
end
end
```

cellocApr.m

```
function [x,y]=cellocApr(z)
[a,b]=size(z);
k=0;
for i=1:a
   for j=1:b
      if z(i,j)==2
         k=k+1;
         x(k)=i;
         y(k)=j;
      end
   end
end
end
```

cellocAs.m

```
function [x,y]=cellocAs(z)
[a,b]=size(z);
k=0;
for i=1:a
   for j=1:b
```

```
        if z(i,j)==1
            k=k+1;
            x(k)=i;
            y(k)=j;
        end
    end
end
end
```

cellocdif.m

```
function [x,y]=cellocdif(z)
if max(max(z))>1
    [a,b]=size(z);
    k=0;
    for i=1:a
        for j=1:b
                k=k+1;
                x(k)=i;
                y(k)=j;
            end
        end
    end
end
if max(max(z))<=1
    x=0;
    y=0;
end
end
```

cellocNoAs.m

```
function [x,y]=cellocNoAs(z)
[a,b]=size(z);
k=0;
for i=1:a
    for j=1:b
        if z(i,j)>=2
            k=k+1;
            x(k)=i;
            y(k)=j;
        end
    end
end
end
```

densityrc.m

```
function [dens]=densityrc(As,frow,fcolumn,denscc)
Asd=zeros(240,170);
As(frow,fcolumn)=0;
r=1;
    for i=1:240
        for j=1:170
            if i<81
            Asd(i,j)=As(i,j);
            end
            if i>80 && i<161
            Asd(i,j)=As(i-80,j);
            end
            if i>160 && i<241
            Asd(i,j)=As(i-160,j);
            end
        end
    end
    if fcolumn<17
    k=1:fcolumn+16;
    end
    if fcolumn>154
    k=fcolumn-16:170;
    end
    if fcolumn >= 17 && fcolumn <=154
    k=fcolumn-16:fcolumn+16;
    end
    l=frow+80-16:frow+80+16;
    densitydivi=zeros(length(l),length(k));
    for m=1:length(l)
        for n=1:length(k)
            if Asd(l(m),k(n))~= 0 &&
distancefun(frow+80,fcolumn,l(m),k(n))<=16
densitydivi(r)=1/((distancefun(frow+80,fcolumn,l(m),k(n))^2)+0
.01);
                r=r+1;
            end
        end
    end
    dens=sum(sum(densitydivi));
end
```

distancecells.m

```
function x=distancecells(y,m,n)
[a,b] = size(y);
for i=1:a
```

```
    for j=1:b
        x(i,j)=sqrt(((m-i)^2)+((n-j)^2));
    end
end
end
```

distancefun.m

```
function x=distancefun(a,b,c,d)
x=sqrt(((a-c)^2)+((b-d)^2));
end
```

division.m

```
function
[Astest,v]=division(As,frow,fcolumn,u,densfordiv,mindensdivmig,maxdensdivmig,denscc,distmax)%,densfac)
clear count
if As(frow,fcolumn)==1
    v=u;
    Astest=As;
    Astest(frow,fcolumn)=0;
    if frow==1
        a=[80,1,2];
    end
    if frow==80
        a=[79,80,1];
    end
    if frow >1 && frow <80
        a= frow-1:frow+1;
    end
    if fcolumn==1
        b=[1,2];
    end
    if fcolumn==170
        b=[169,170];
    end
    if fcolumn>1 && fcolumn <170
        b=fcolumn-1:fcolumn+1;
    end
    Densdiv=zeros(length(a),length(b));
    densidivi=ones(80,170);
    for i=1:length(a)
        for j=1:length(b)

Densdiv(i,j)=densityrc(Astest,a(i),b(j),densidivi);%,densfac);
            if a(i)==frow && b(j)==fcolumn
                Densdiv(i,j)=100;
            end
        end
    end
    [c,I]=min(Densdiv);
    [d,J]=min(min((Densdiv)));
    if min(min(Densdiv)) <= densfordiv
        Astest=As;
        Astest(a(I(J)),b(J))=1;
        mrow=a(I(J));
        mcolumn=b(J);
        count=0;
        Asmig=Astest;
        for i=1:distmax
[Asmig,mrow,mcolumn]=migrationdiv(Asmig,mrow,mcolumn,mindensdivmig,maxdensdivmig,denscc);
[Asmig,frow,fcolumn]=migrationdiv(Asmig,frow,fcolumn,mindensdivmig,maxdensdivmig,denscc);
            if isequal(Asmig,Astest)~=1
                count=count+1;
                imwrite(Asmig/16,num2str(u),'png');
                v=v+1;
            end
            Astest=Asmig;
        end
        if count < 2
            Astest=As;
        end
        imwrite(Astest/16,num2str(v),'png');
        v=v+1;
    end
    if min(min(Densdiv)) > densfordiv
        Astest=As;
         imwrite(Astest/16,num2str(v),'png');
         v=v+1;
    end
end
if As(frow,fcolumn)> 1 && As(frow,fcolumn)<16
    v=u;
    Astest=As;
    Astest(frow,fcolumn)=As(frow,fcolumn)*2;
    display('gmh');
end
if As(frow,fcolumn)>=16
```

```
    v=u;
    Astest=As;
    Astest(frow,fcolumn)=16;
    display('gmh1')
        imwrite(Astest/16,num2str(v),'png');
        v=v+1;
end
end
```

divisionr.m

```
function [As,u]=
divisionr(Bs,difftag,divr,u,densfordiv,mindensdivmig,maxdensdi
vmig,denscc)%,densfac)
As=Bs;
[rowAss,columnAss]=celllocation(As);
randcds=rand(1,length(rowAss));
rans=zeros(1,length(rowAss));
for a=1:length(rowAss)
    [maxim,rans(a)]=max(randcds);
    randcds(rans(a))=0;
end
ff=round(divr*length(rans));
for a=1:ff
    if difftag(rowAss(rans(a)),columnAss(rans(a)))~= 1 &&
As(rowAss(rans(a)),columnAss(rans(a)))==1

[As,u]=division(As,rowAss(rans(a)),columnAss(rans(a)),u,densf
ordiv,mindensdivmig,maxdensdivmig,denscc,6);
        imwrite(As/16,num2str(u),'png');
        u=u+1;
    end
    if difftag(rowAss(rans(a)),columnAss(rans(a)))== 1
        if As(rowAss(rans(a)),columnAss(rans(a)))<16
            As(rowAss(rans(a)),columnAss(rans(a)))= 2*
As(rowAss(rans(a)),columnAss(rans(a)));
            imwrite(As/16,num2str(u),'png');
            u=u+1;
        end
    end
end
end
```

migratesort.m

```
function
[rowAsort,columnAsort]=migratesort(As,rowAs,columnAs)
DensityS=zeros(1,length(rowAs));
densum=zeros(240,170);
Astrial=As;
rowAst=zeros(1,length(rowAs)*3);
columnAst=zeros(1,length(columnAs)*3);
rowAst(1:length(rowAs))=rowAs;
rowAst(length(rowAs)+1:2*length(rowAs))=rowAs+80;
rowAst((length(rowAs)*2)+1:3*length(rowAs))=rowAs+160;
columnAst(1:length(columnAs))=columnAs;
columnAst(length(columnAs)+1:2*length(columnAs))=column
As;
columnAst((length(columnAs)*2)+1:3*length(columnAs))=colu
mnAs;
for i=1:length(columnAst)
    Astrial(rowAst(i),columnAst(i))=0;
    Astrials=zeros(240,170);
    for m=1:240
        for n=1:170
            if m<81
                Astrials(m,n)=Astrial(m,n);
            end
            if m>80 && m<161
                Astrials(m,n)=Astrial(m-80,n);
            end
            if m>160 && m<241
                Astrials(m,n)=Astrial(m-160,n);
            end
        end
    end
    denind=zeros(1,length(rowAst));
    for j=1:length(rowAst)
     denind(j) =
(1/((distancefun(rowAst(i),columnAst(i),rowAst(j),columnAst(j)
)^2)+0.01));
        if denind(j)>90
            denind(j)=0;
        end
    end
    densum(rowAst(i),columnAst(i))=sum(denind);
    Astrial=As;
end
DensityOrd=zeros(80,170);
for i=1:80
    for j=1:170
        DensityOrd(i,j)=densum(i+80,j);
```

```
    end
end
for i=1:length(rowAs)
    DensityS(i)=DensityOrd(rowAs(i),columnAs(i));
end
rowAsort=zeros(1,length(rowAs));
columnAsort=zeros(1,length(columnAs));
for i=1:length(rowAs)
    [c,I]=max(DensityS);
    rowAsort(i)=rowAs(I);
    columnAsort(i)=columnAs(I);
    DensityS(I)=0;
end
end
```

migration.m

```
function
[Astest]=migration(As,frow,fcolumn,mindensmig,maxdensmig,
Qsr)
denmigs=ones(80,170);
denscell=densityrc(As,frow,fcolumn,denmigs);%,densfac);
if denscell >= mindensmig
    if As(frow,fcolumn)==1
        Astest=As;
        Astest(frow,fcolumn)=0;
        if frow==1
            a=[80,1,2];
        end
        if frow==80
            a=[79,80,1];
        end
        if frow >1 && frow <80
            a= frow-1:frow+1;
        end
        if fcolumn==1
            b=[1,2];
        end
        if fcolumn==170
            b=[169,170];
        end
        if fcolumn>1 && fcolumn <170
            b=fcolumn-1:fcolumn+1;
        end
        Densdiv=zeros(length(a),length(b));
        for i=1:length(a)
            for j=1:length(b)
Densdiv(i,j)=densityrc(Astest,a(i),b(j),Qsr);%,densfac);
                if Astest(a(i),b(j))==1 %&& a(i)~=frow &&
b(j)~=fcolumn
                    Densdiv(i,j)=100;
                end
            end
        end
        if sum(sum(Densdiv))~=0 && min(min(Densdiv))<
maxdensmig
            [c,I]=min(Densdiv);
            [d,J]=min(min((Densdiv)));
            Astest=As;
            Astest(frow,fcolumn)=0;
            Astest(a(I(J)),b(J))=1;
        end
        if sum(sum(Densdiv))==0
            Astest(frow,fcolumn)=1;
        end
    end
    if As(frow,fcolumn)~=1
        Astest=As;
    end
end
if denscell<mindensmig
    Astest=As;
end
end
```

migrationdiv.m

```
function
[Astest,mrow,mcolumn]=migrationdiv(As,frow,fcolumn,minden
sdivmig,maxdensdivmig,denscc)
denmigs=ones(80,170);
denmd=densityrc(As,frow,fcolumn,denmigs);
if denmd >= mindensdivmig
    if As(frow,fcolumn)==1
        Astest=As;
        Astest(frow,fcolumn)=0;
        if frow==1
            a=[80,1,2];
        end
        if frow==80
            a=[79,80,1];
        end
```

```
    if frow >1 && frow <80
       a= frow-1:frow+1;
    end
    if fcolumn==1
       b=[1,2];
    end
    if fcolumn==170
       b=[169,170];
    end
    if fcolumn>1 && fcolumn <170
       b=fcolumn-1:fcolumn+1;
    end
    Densdiv=zeros(length(a),length(b));
    for i=1:length(a)
       for j=1:length(b)

Densdiv(i,j)=densityrc(Astest,a(i),b(j),denscc);%,densfac);
            if Astest(a(i),b(j))==1 %&& a(i)~=frow &&
b(j)~=fcolumn
                Densdiv(i,j)=100;
            end
       end
    end
    if sum(sum(Densdiv))~=0
       [c,I]=min(Densdiv);
       [d,J]=min(min((Densdiv)));
       if min(min(Densdiv))>=maxdensdivmig
          Astest=As;
          Astest(frow,fcolumn)=0;
          Astest(a(I(J)),b(J))=1;
          mrow=a(I(J));
          mcolumn=b(J);
       end
       if min(min(Densdiv))<maxdensdivmig
          Astest=As;
          mrow=frow;
          mcolumn=fcolumn;
       end
    end
    if sum(sum(Densdiv))==0
       Astest(frow,fcolumn)=1;
       mrow=frow;
       mcolumn=fcolumn;
       end
    end
end
if denmd<mindensdivmig
    Astest=As;
    mrow=frow;
    mcolumn=fcolumn;
    display('deejayyyy');
end
end
```